distribution of PC3, do not show a corresponding spectral change. If the cell was able to break down the hemozoin biocrystals, we would expect to see a change in the spectra to reflect the heme components (*e.g.* hemin), which are spectrally distinct from hemozoin.[24] The relative stability of the hemozoin spectra indicates that the cell is unable to breakdown the hemozoin within the five hour time period observed in this study. Consistent with this finding, it has also been observed that hemozoin outside the cell is resistant to degradation by a number of acids, peroxides *etc.* and it is therefore assumed that hemozoin is similarly not broken down by such chemicals within the phagosome/lysosome.[47] We also measured the hemozoin spectra under varying pH conditions and did not find a significant pH dependence of the spectra, confirming that the spectral changes observed are not related to differing pH environments within the cell (ESI S3†).

Since the hemozoin does not appear to be broken down, lysosomal compartments could become overloaded resulting in lysosomal dysfunction and lysosome membrane permeabilization (LMP).[48] Partial LMP can result in the generation of reactive oxygen species (ROS)[48] which is a known inducer of cellular inflammatory pathways, for example the NLRP3 inflammasome,[49–51] while massive LMP will result in the release of the lysosomal contents into the cytoplasm, triggering conditions such as oxidative stress and inflammation, ultimately resulting in the induction of cell death pathways.[48] These processes would be expected to occur over longer time scales than were studied in our experiments, and observation over later time steps should provide additional findings. However, we focused on the initial uptake over the time scale where hemozoin should reach the lysosomes. This time scale also precludes the chance that hemozoin had already been processed and ejected from another macrophage before being phagocytosed by the macrophage under observation, which could occur at longer time scales.

Conclusions

The macrophage response to hemozoin mediates inflammation and some of the detrimental effects of malaria infection. The chemical specificity of the label-free Raman measurements show that the spatial information provided by the imaging mode is essential for observing the location and dynamics of hemozoin and the corresponding changes in macrophages. The additional discrimination of multiple hemozoin components in the input samples and their different fates within the cell is a key factor in understanding the role of hemozoin in the immune response. This will be an important step to solving some of the still unknown questions that concern innate immune responses which occur during malaria.

Macrophages engulf hemozoin upon exposure, and hemozoin was observed in an inhomogeneous distribution throughout the cytoplasm. Hemozoin was not observed to enter the nucleus, but in the cytoplasm, inclusion of hemozoin causes a rearrangement of the endogenous molecules in the cell. The macrophage cells also increase in size and large vacuoles appear. Although intuitive in the sense that cellular molecules cannot exist where hemozoin nanocrystals exist, the extent to which hemozoin forced the exclusion of cellular content was not expected. This type of study is an ideal target for Raman imaging analysis, since it readily separates contributions from the cell as a whole into discrete spectral components. The large holes observed in the PCA analysis (PC2) preclude significant co-localization of hemozoin with other molecules.

The hemozoin samples measured *in vitro* were found to contain two components, which were similarly observed in the cells. One hemozoin component is anti-correlated with a lipid-based change in the cell: a transient lipid response which occurs around 3 hours, then decreases by 5 hours. We attribute the lipid-rich components to the plasma membranes involved in the phagocytosis of hemozoin particles, followed by fusion with lysosomes. From our results, it also appears that neither type of hemozoin is degraded by the macrophage within the time period studied here. The subsequent increase in hemozoin fractions can then be attributed to the build-up of hemozoin within the lysosomes as a result of its poor degradability.

There are a number of contradictory reports on whether the presence of hemozoin results in up- or down-regulation of the immune response.[6,47] These could, in part, be explained by different types of hemozoin or the inclusion of additional molecules in the hemozoin preparation.[7,8,10] Many reports using hemozoin do not measure the spectra and those that do, to our knowledge, have measured hemozoin reference spectra without consideration of the spatial distribution, or whether the hemozoin reference is uniform. Our reference spectrum from the hemozoin preparation (ESI S2†) clearly shows two spectral components which are spatially isolated. The reason for this is not clear but it is worth noting that the same is likely to be true in other experiments using synthetic (and perhaps also from parasite-derived) hemozoin. The close match between these two hemozoin components and the principal components observed in the multivariate analysis shows that the two components in the reference spectra do not appear to be changed by the cell. The fact that these two components in the cell are not co-localized additionally hints that they are subject to different processes within the cell.

Acknowledgements

The authors would like to thank Y. Igari and K. Ohata for the preparation of synthetic hemozoin. We acknowledge funding from the Japan Society for the Promotion of Science (JSPS) through the Funding Program for World-Leading Innovative R&D on Science and Technology (FIRST Program), JSPS World Premier International Research Center Initiative Funding Program, the Japan Science and Technology PRESTO program and from the Photonics Center, Osaka University, under the program of MEXT Photonics Advanced Research Center Program.

Notes and references

1 G. Newton, *The global problem at a glance*, http://malaria.wellcome.ac.uk/doc.WTD022247.html, Wellcome Trust, 2006.
2 K. Mendis, B. J. Sina, P. Marchesini and R. Carter, *Am. J. Trop. Med. Hyg.*, 2001, **64**, 97–106.
3 L. R. Moore, H. Fujioka, P. S. Williams, J. J. Chalmers, B. Grimberg, P. a. Zimmerman and M. Zborowski, *FASEB J.*, 2006, **20**, 747–749.
4 C. Coban, K. J. Ishii, T. Horii and S. Akira, *Trends Microbiol.*, 2007, **15**, 271–278.
5 D. J. Perkins, T. Were, G. C. Davenport, P. Kempaiah, J. B. Hittner and J. M. Ong'echa, *Int. J. Biol. Sci.*, 2001, **7**, 1427–1442.
6 E. M. Riley and V. A. Stewart, *Nat. Med.*, 2013, **19**, 168–178.
7 M. T. Shio, F. a. Kassa, M.-J. Bellemare and M. Olivier, *Microbes Infect.*, 2010, **12**, 889–899.
8 C. Coban, M. Yagi, K. Ohata, Y. Igari, T. Tsukui, T. Horii, K. J. Ishii and S. Akira, *Allergol. Int.*, 2010, **59**, 115–124.
9 P. Perlmann and M. Troye-Blomberg, *Chem. Immunol.*, 2002, **80**, 229–242.
10 P. Parroche, F. N. Lauw, N. Goutagny, E. Latz, B. G. Monks, A. Visintin, K. A. Halmen, M. Lamphier, M. Olivier, D. C. Bartholomeu, R. T. Gazzinelli and D. T. Golenbock, *Proc. Natl. Acad. Sci. U. S. A.*, 2007, **6**, 1919–1924.
11 M. Jaramillo, M.-J. Bellemare, C. Martel, M. T. Shio, A. P. Contreras, M. Godbout, M. Roger, E. Gaudreault, J. Gosselin, D. S. Bohle and M. Olivier, *PloS One*, 2009, **4**, e6957.
12 C. Coban, Y. Igari, M. Yagi, T. Reimer, S. Koyama, T. Aoshi, K. Ohata, T. Tsukui, F. Takeshita, K. Sakurai, T. Ikegami, A. Nakagawa, T. Horii, G. Nuñez, K. J. Ishii and S. Akira, *Cell Host Microbe*, 2010, **7**, 50–61.
13 T. Hänscheid, T. J. Egan and M. P. Grobusch, *Lancet Infect. Dis.*, 2007, **7**, 675–685.
14 E. Schwarzer, F. Turrini, D. Ulliers, G. Giribaldi, H. Ginsburg and P. Arese, *J. Exp. Med.*, 1992, **176**, 1033–1041.
15 C. Krafft, S. B. Sobottka, G. Schackert and R. Salzer, *Analyst*, 2005, **130**, 1070–1077.
16 M. Miljković, T. Chernenko, M. J. Romeo, B. Bird, C. Matthäus and M. Diem, *Analyst*, 2010, **135**, 2002–2013.
17 A. Ghita, F. C. Pascut, M. Mather, V. Sottile and I. Notingher, *Anal. Chem.*, 2012, **84**, 3155–3162.
18 K. Lau, A. Hobro, T. Smith, T. Thurston and B. Lendl, *Vib. Spectrosc.*, 2012, **60**, 34–42.
19 S. M. Ali, F. Bonnier, H. Lambkin, K. Flynn, V. McDonagh, C. Healy, T. C. Lee, F. M. Lyng and H. J. Byrne, *Anal. Methods*, 2013, **5**, 2281–2291.
20 T. Frosch, S. Koncarevic, K. Becker and J. Popp, *Analyst*, 2009, **134**, 1126–1132.
21 R. Puntharod, G. T. Webster, M. Asghari-Khiavi, K. R. Bambery, F. Safinejad, S. Rivadehi, S. J. Langford, K. J. Haller and B. R. Wood, *J. Phys. Chem. B*, 2010, **114**, 12104–12115.
22 A. Bonifacio, S. Finaurini, C. Krafft, S. Parapini, D. Taramelli and V. Sergo, *Anal. Bioanal. Chem.*, 2008, **392**, 1277–1282.
23 B. R. Wood, A. Hermelink, P. Lasch, K. R. Bambery, G. T. Webster, M. A. Khiavi, B. M. Cooke, S. Deed, D. Naumann and D. McNaughton, *Analyst*, 2009, **134**, 1119–1125.
24 A. J. Hobro, A. Konishi, C. Coban and N. I. Smith, *Analyst*, 2013, **138**, 3927–3933.
25 W. Kim, S. K. Ozdemir, J. Zhu, M. Faraz, C. Coban and L. Yang, *Opt. Express*, 2012, **20**, 29426–29446.
26 N. Pavillon, K. Bando, K. Fujita and N. I. Smith, *J. Biophotonics*, 2013, **6**, 587–597.
27 K. Hamada, K. Fujita, N. I. Smith, M. Kobayashi, Y. Inouye and S. Kawata, *J. Biomed. Opt.*, 2013, **13**, 044027.
28 D. F. H. Wallach, S. P. Verma and J. Fookson, *Biochim. Biophys. Acta*, 1979, **559**, 153–208.
29 G. J. Thomas and K. A. Hartman, *Biochim. Biophys. Acta*, 1973, **312**, 311–322.
30 K. Pearson, *Philos. Mag. Ser. 6*, 1901, **2**, 559–572.
31 M. Okada, N. I. Smith, A. F. Palonpon, H. Endo, S. Kawata, M. Sodeoka and K. Fujita, *Proc. Natl. Acad. Sci. U. S. A.*, 2012, **109**, 28–32.
32 Y. Guan and G. J. Thomas, *J. Mol. Struct.*, 1996, **379**, 31–41.
33 A. J. Hobro, D. M. Standley, S. Ahmad and N. I. Smith, *Phys. Chem. Chem. Phys.*, 2013, **15**, 13199–13208.
34 S. C. Erfurth, E. J. Kiser and W. L. Peticolas, *Proc. Natl. Acad. Sci. U. S. A.*, 1972, **69**, 938–941.
35 A. Barth and C. Zscherp, *Q. Rev. Biophys.*, 2002, **35**, 369–430.
36 L. Ashton, A. Hobro, G. L. Conn, M. Rouhi and E. W. Blanch, *J. Mol. Struct.*, 2008, **883–884**, 187–194.
37 J. D. Gelder, K. D. Gussem, P. Vandenabeele and L. Moens, *J. Raman Spectrosc.*, 2007, **38**, 1133–1147.
38 D. I. Ellis, D. P. Cowcher, L. Ashton, S. O'Hagan and R. Goodacre, *Analyst*, 2013, **138**, 3871–3884.
39 R. Schmidt-Ullrich, S. P. Verma and D. F. H. Wallach, *Biochim. Biophys. Acta*, 1976, **426**, 477–488.
40 J. De Gelder, K. De Gussem, P. Vandenabeele, M. Vancanneyt, P. De Vos and L. Moens, *Anal. Chim. Acta*, 2007, **603**, 167–175.
41 G. Socrates, *Infrared and Raman characteristic group frequencies*, Wiley, 3rd edn, 2001.
42 S. Rabinowitz, H. Horstmann, S. Gordon and G. Griffiths, *J. Cell Biol.*, 1992, **116**, 95–112.
43 M. T. Tassin, T. Lang, J. C. Antoine, R. Hellio and A. Ryter, *Eur. J. Cell Biol.*, 1990, **52**, 219–228.
44 M. J. Geisow, P. D. Hart and M. R. Young, *J. Cell Biol.*, 1981, **89**, 645–652.
45 G. L. Lukacs, O. D. Rotstein and S. Grinstein, *J. Biol. Chem.*, 1991, **266**, 24540–24548.
46 J. A. Mindell, *Annu. Rev. Physiol.*, 2012, **74**, 69–86.
47 M. Boura, R. Frita, A. Góis, T. Carvalho and T. Hänscheid, *Trends Parasitol.*, 2013, **29**, 469–476.

48 S. T. Stern, P. P. Adiseshaiah and R. M. Crist, *Part. Fibre Toxicol.*, 2012, **9**, 20.
49 T. Misawa, M. Takahama, T. Kozaki, H. Lee, J. Zou, T. Saitoh and S. Akira, *Nat. Immunol.*, 2013, **14**, 454–460.
50 M. T. Shio, M. Tiemi Shio, S. C. Eisenbarth, M. Savaria, A. F. Vinet, M.-J. Bellemare, K. W. Harder, F. S. Sutterwala, D. S. Bohle, A. Descoteaux, R. a. Flavell and M. Olivier, *PLoS Pathog.*, 2009, **5**, e1000559.
51 C. Dostert, G. Guarda, J. F. Romero, P. Menu, O. Gross, A. Tardivel, M.-L. Suva, J.-C. Stehle, M. Kopf, I. Stamenkovic, G. Corradin and J. Tschopp, *PloS One*, 2009, **4**, e6510.

CellPress

Immunity
Article

The Enzyme Cyp26b1 Mediates Inhibition of Mast Cell Activation by Fibroblasts to Maintain Skin-Barrier Homeostasis

Yosuke Kurashima,[1,2,3,4] Takeaki Amiya,[1,2,4,5] Kumiko Fujisawa,[1,2] Naoko Shibata,[1,2,4,5] Yuji Suzuki,[1] Yuta Kogure,[1,4,5] Eri Hashimoto,[1,4] Atsushi Otsuka,[6] Kenji Kabashima,[6] Shintaro Sato,[1,2] Takeshi Sato,[1,4,5] Masato Kubo,[7,8] Shizuo Akira,[9] Kensuke Miyake,[3] Jun Kunisawa,[1,2,4,5,10,11,*] and Hiroshi Kiyono[1,2,5,10,*]

[1]Division of Mucosal Immunology, Department of Microbiology and Immunology, The Institute of Medical Science, The University of Tokyo, Tokyo 108-8639, Japan

[2]Core Research for Evolutional Science and Technology, Japan Science and Technology Agency, Tokyo 102-0075, Japan

[3]Division of Innate Immunity, Department of Microbiology and Immunology, The Institute of Medical Science, The University of Tokyo, Tokyo 108-8639, Japan

[4]Laboratory of Vaccine Materials, National Institute of Biomedical Innovation, Osaka 567-0085, Japan

[5]Department of Medical Genome Science, Graduate School of Frontier Science, The University of Tokyo, Chiba 277-8561, Japan

[6]Department of Dermatology, Kyoto University Graduate School of Medicine, Kyoto 606-8501, Japan

[7]Laboratory for Cytokine Regulation, Research Center for Integrative Medical Science, RIKEN Yokohama Institute, Kanagawa 230-0045, Japan

[8]Division of Molecular Pathology, Research Institute for Biological Sciences, Tokyo University of Sciences, Chiba 278-0022, Japan

[9]Laboratory of Host Defense, WPI Immunology Frontier Research Center, Osaka University, Osaka 565-0871, Japan

[10]International Research and Development Center for Mucosal Vaccines, The Institute of Medical Science, The University of Tokyo, Tokyo 108-8639, Japan

[11]Department of Microbiology and Immunology, Kobe University School of Medicine, Kobe 650-0017, Japan

*Correspondence: kunisawa@nibio.go.jp (J.K.), kiyono@ims.u-tokyo.ac.jp (H.K.)

http://dx.doi.org/10.1016/j.immuni.2014.01.014

SUMMARY

Mast cells (MCs) mature locally, thus possessing tissue-dependent phenotypes for their critical roles in both protective immunity against pathogens and the development of allergy or inflammation. We previously reported that MCs highly express P2X7, a receptor for extracellular ATP, in the colon but not in the skin. The ATP-P2X7 pathway induces MC activation and consequently exacerbates the inflammation. Here, we identified the mechanisms by which P2X7 expression on MCs is reduced by fibroblasts in the skin, but not in the other tissues. The retinoic-acid-degrading enzyme Cyp26b1 is highly expressed in skin fibroblasts, and its inhibition resulted in the upregulation of P2X7 on MCs. We also noted the increased expression of P2X7 on skin MCs and consequent P2X7- and MC-dependent dermatitis (so-called retinoid dermatitis) in the presence of excessive amounts of retinoic acid. These results demonstrate a unique skin-barrier homeostatic network operating through Cyp26b1-mediated inhibition of ATP-dependent MC activation by fibroblasts.

INTRODUCTION

Mast cells (MCs) produce inflammatory mediators to initiate and exacerbate inflammation (Gilfillan and Beaven, 2011; Tsai et al., 2011). Therefore, depletion or inhibition of activated MCs attenuates the inflammatory reactions (Feyerabend et al., 2011; Otsuka et al., 2011). MCs are activated by various stimuli such as allergen-immunoglobulin E (IgE) complex and high-affinity IgE receptor (FcεRI) pathway, and molecules released from necrotic cells (e.g., IL-33) after tissue injury in various inflammatory conditions (Lunderius-Andersson et al., 2012). Furthermore, previous findings, including ours, suggest that extracellular ATP acts as a danger signal to MCs and initiates inflammation (Kurashima et al., 2012; Sudo et al., 1996). Extracellular ATP is released in response to various stresses including shear, osmolality, oxidative, and inflammatory one (Junger, 2011). Local ATP injection into the skin induces ear swelling (Mizumoto et al., 2002). Furthermore, ATP amounts are increased in the extracellular compartment in irritant contact dermatitis associated with zinc-deficiency (Kawamura et al., 2012; Mizumoto et al., 2002). In addition to skin inflammation, increased ATP concentrations are also found in asthma, graft-versus-host disease, and inflammatory bowel disease (Idzko et al., 2007; Wilhelm et al., 2010; Kurashima et al., 2012). To resolve inflammation, the extracellular ATP is degraded by the ectonucleoside triphosphate diphosphohydrolase CD39 expressed on immune cells such as Langerhans cells (LCs) and regulatory T cells (Junger, 2011). Therefore, inflammation is exacerbated in CD39-deficient mice because of increased local ATP concentration (Mizumoto et al., 2002).

As receptors for extracellular ATP, P2 purinoceptors comprise P2X1 to P2X7 and act as ATP-gated ion channels (Di Virgilio, 2007). P2X7 is involved in various inflammations and thus inflammation associated with graft-versus-host disease and colonic inflammation are ameliorated by P2X7 inhibition (Kurashima et al., 2012; Wilhelm et al., 2010). In addition,

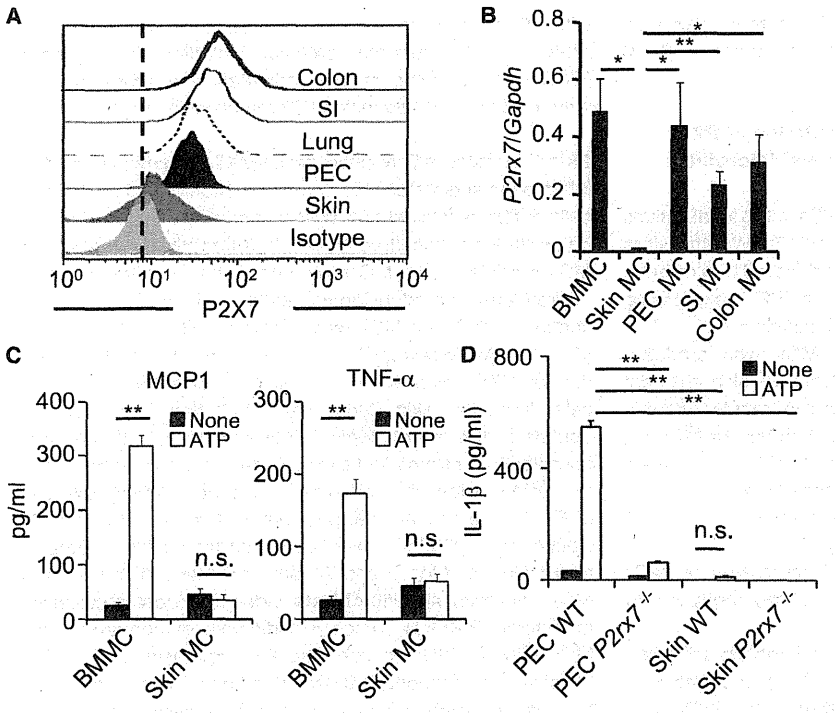

Figure 1. Low P2X7 Expression on Skin Mast Cells

(A) P2X7 expression on MCs in the colon, small intestine (SI), lung, peritoneal cavity (PEC), and skin was measured by flow cytometry. "Isotype" indicates isotype IgG2b staining as a negative control. Data are representative of at least six independent experiments.

(B) Gene expression of *P2rx7* in sorted MCs from various tissues was examined by quantitative RT-PCR. Data are means ± SEM (n = 4). *p < 0.05; **p < 0.01.

(C) Production of MCP1 and TNF-α in culture supernatant was determined after stimulation of bone-marrow-derived MCs (BMMCs) or skin MCs with 0.5 mM ATP. Data are shown as means ± SEM (n = 3). **p < 0.01; n.s., not significant.

(D) IL-1β production was measured by ELISA after sorted MCs from WT or *P2rx7*$^{-/-}$ mice were stimulated with LPS with or without ATP (n = 3). **p < 0.01; n.s., not significant.

cathelicidin-derived peptide LL37 directly stimulates P2X7 and induces skin inflammation such as psoriasis and rosacea (Elssner et al., 2004; Yamasaki et al., 2007). Despite such researches, little is understood about the regulatory mechanisms of P2X7 expression.

We previously generated an anti-P2X7 monoclonal antibody and revealed that P2X7 is highly expressed on colonic MCs, which is associated with the aggravation of intestinal inflammation (Kurashima et al., 2012). We simultaneously observed that skin MCs have lower—or almost no—expression of P2X7 (Kurashima et al., 2012). Intriguingly, it was reported that excessive production of IL-1β in skin MCs as a result of constitutive activation of NOD-like receptor family, pyrin domain-containing 3 (one of the signal pathways of P2X7), causes skin inflammation (Nakamura et al., 2012). These observations suggest that ectopic expression and aberrant activation of P2X7 in MCs might elicit skin inflammation. Here, we identified the unique regulatory function of skin fibroblasts in producing the retinoic acid (RA)-degrading enzyme Cyp26b1 to inhibit P2X7 expression on MCs for maintaining the skin homeostasis. Furthermore, we provide evidence that disruption of Cyp26b1-mediated regulatory function of skin fibroblasts, together with commensal microbial stimulation, induced the development of P2X7- and MC-mediated severe dermatitis.

RESULTS

Low P2X7 Expression by Skin MCs Accounts for Insensitivity to Extracellular ATP

We initially confirmed that skin c-kit$^+$ FcεRIα$^+$ cells were MCs by their selective depletion by diphtheria toxin (DT) treatment of MaS-TRECK mice where DT receptor (DTR) was specifically expressed on MCs (see Figure S1A available online) (Sawaguchi et al., 2012). In our previous study, P2X7 is expressed on MCs in the colon but low or undetectable in skin MCs (Kurashima et al., 2012). When we further compared P2X7 expression on MCs among colon, small intestine, lung, peritoneal cavity (PEC), and skin, it was lower on skin MCs than on MCs in the other tissues (Figure 1A). To assess whether the lower P2X7 expression on skin MCs was due to low expression at transcription or posttranscriptional events, we performed RT-PCR and intracellular flow cytometry analysis. Gene expression encoding P2X7 (*P2rx7*) was low on skin MCs, but not on MCs from the other tissues (Figure 1B). Consistently, the intracellular expression of P2X7 protein was also low in skin MCs (Figure S1B).

MCs can be categorized into two types—connective tissue and mucosal—in terms of protease phenotype. Connective-tissue-type MCs are located mainly in the skin and PEC and express mast cell protease (Mcpt) 4 and 5 (Gurish and Austen, 2012). Mucosal-type MCs are located in the gastroenterological mucosa and express Mcpt2 (Xing et al., 2011). Quantitative RT-PCR (qRT-PCR) and gene-microarray analyses indicated that even though the protease expression patterns were identical to those in previous observations (Figure S1C), P2X7 expression patterns were not applicable to the current two MC subtypes (Figure S1D).

To examine the reactivity of skin MCs against extracellular ATP, we stimulated them with ATP and measured the production of tumor necrosis factor alpha (TNF-α) and MCP1. In accordance with the lack of P2X7 expression on skin MCs, production of TNF-α and MCP1 upon ATP stimulation was detected in bone-marrow-derived MCs (BMMCs), but not skin MCs (Figure 1C). P2X7 plays a pivotal role in inflammasome activation along with stimulation by bacterial components such as lipopolysaccharide (LPS); these actions lead to interleukin-1β (IL-1β) production (Di Virgilio, 2007). Thus, IL-1β production was noted when PEC MCs from wild-type (WT) but not *P2rx7*$^{-/-}$ mice

were stimulated with both LPS and ATP. In contrast, skin MCs from both WT and *P2rx7*$^{-/-}$ mice did not produce IL-1β (Figure 1D).

Skin Environment-Mediated Downregulation of P2X7 Expression Is Independent of Commensal Microbiota and Immune Cells

MC progenitors differentiate into mature MCs in the local tissues (Gurish and Austen, 2012; Xing et al., 2011). We therefore considered that P2X7 expression would be affected by skin environment. To test this possibility, we transferred P2X7-expressing (WT) BMMCs directly into the skin of MC-deficient *Kit*$^{W\text{-}sh/W\text{-}sh}$ mice. P2X7 expression on transferred MCs was gradually decreased to identical expression to those of skin resident MCs in WT mice within 10 days after adoptive transfer (Figures 2A and 2B). Furthermore, long-term reconstitution of MCs via the intravenous and intraperitoneal routes in *Kit*$^{W\text{-}sh/W\text{-}sh}$ mice led to successful reconstitution of P2X7-expressing MCs in the PEC and colon, whereas MCs in the skin showed low P2X7 expression (Figure S2A; data not shown) (Kurashima et al., 2012). These results indicated that P2X7 expression on MCs was reversible which was directly and negatively regulated by the skin environment.

It was recently shown that commensal microbiota stimulate immune responses in the skin (Naik et al., 2012), allowing us to compare P2X7 expression in specific-pathogen-free (SPF) and germ-free (GF) mice and in mice lacking MyD88, an adaptor molecule of an innate sensor for bacterial components (e.g., toll-like receptors [TLRs]). The low P2X7 expression on skin MCs was maintained in these mice (Figures 2C and D), suggesting that commensal microbiota did not directly influence P2X7 expression on skin MCs.

Various unique immune cells, such as γδ T cells and LCs, are important for maintaining skin homeostasis (Di Meglio et al., 2011). To examine the contribution of immune cells to the reduction of P2X7 on skin MCs, we analyzed mice lacking T cells (*Tcrb*$^{-/-}$*TCRd*$^{-/-}$), B cells (*Ighm*$^{-/-}$), or both (*Rag1*$^{-/-}$). Identically low P2X7 expression was seen on skin MCs of these mice (Figures 2C and 2E). To further explore the involvement of other immune cells, we analyzed DT-treated *Itgax*-DTR mice (Jung et al., 2002) and *Id2*$^{-/-}$ mice (Hacker et al., 2003), which lack dendritic cells (DCs) and LCs, respectively. No change of P2X7 expression on skin MCs was noted in the absence of DCs or LCs (Figures 2C and 2F). Also, the P2X7 expression in the colon MCs was comparable among these gene-deficient and WT mice (data not shown). Thus, T and B cells, DCs, and LCs were dispensable for the downregulation of P2X7 expression on skin MCs.

The skin possesses inhibitory cytokines, vitamins, and lipid mediators (Biggs et al., 2010; Schirmer et al., 2010). For instance, vitamin D_3 and IL-10 play regulatory roles in skin inflammation (Biggs et al., 2010). Although IL-10 receptor expression on MCs was slightly higher in skin than in colon (Figure 2G), no changes of P2X7 expression were noted on MCs supplemented with 1α,25$(OH)_2D_3$ (an active metabolite of vitamin D_3) or in *Il10*$^{-/-}$ mice (Figure S2B; Figure 2H). We also assessed the involvement of prostaglandin E2 (PGE_2), another candidate for control of skin MC functions (Gilfillan and Beaven, 2011). P2X7 expression on BMMCs was not altered when they were treated with PGE_2, indomethacin, or pertussis toxin, an inhibitor of G protein-coupled receptor pathway including PGE_2 receptors (Figure S2C). These results indicated that these mediators were redundant in regulating P2X7 expression on MCs.

Skin Fibroblasts Downregulate P2X7 Expression on MCs

It has been suggested that communication of MCs with stromal cells or fibroblasts induces optimal and tissue-dependent maturation. Indeed, coculture of skin 3T3 fibroblasts with immature MCs modulates the MC phenotypes, such as the expression of proteases and adhesion molecules (Takano et al., 2008). We confirmed that skin MCs were localized with fibroblasts in vivo (Figure S3A). To test the involvement of fibroblasts in the regulation of P2X7 expression, we isolated fibroblasts or stromal cells from the skin, lung, small intestine, and colon. We confirmed the morphological characteristics of tissue-derived fibroblasts or stromal cells (e.g., bipolar or multipolar) and their elongated shape with adherent growth together with expression of ER-TR7, a stromal cell pan-marker (Figures S3B and S3C). Coculture of BMMCs with colon stromal cells induced the expression of *Mcpt1* and *Mcpt2*, indicative of mucosal-type MCs; whereas skin fibroblasts induced *Mcpt4* expression in cocultured BMMCs, which is indicative of connective tissue MCs (Figure S3D). In contrast, the expression of FcεRIα on MCs was not changed in these conditions (Figure S3D). In addition, morphological and biochemical analyses revealed that skin fibroblasts regulated the expression of secretory granule components, such as heparin and chondroitin sulfate, in the cocultured MCs (Figure S3E); this behavior is characteristics of connective-tissue-type MCs (Gurish and Austen, 2012). These results indicated that coculture with stromal cells or fibroblasts induced the terminally differentiated and local-environment-adjusted MCs.

Under these experimental conditions, skin fibroblasts inhibited the P2X7 expression on cocultured BMMCs (Figures 3A and 3B). However, stromal cells from the colon and small intestine did not suppress their P2X7 expression (Figures 3A and 3B). In the case of coculture with lung-derived fibroblasts, P2X7 expression was partially suppressed, but the suppression was weaker than that with skin fibroblasts (Figures 3A and 3B). Interestingly, inhibition of P2X7 expression still occurred when both cell types were separately cultured in a transwell culture system (Figure 3C), suggesting that secretory factors from the skin fibroblasts are capable of reducing the P2X7 expression on MCs. Because MCs were differentiated from MC progenitors (Gurish and Austen, 2012), we cocultured BM cells containing MC progenitors with either skin fibroblasts or colon stromal cells for 2 to 3 weeks. P2X7 expression on newly differentiated MCs was detected in the presence of colonic stromal cells, whereas their P2X7 expression was decreased in the presence of skin fibroblasts (Figure 3D). Furthermore, P2X7 expression recovered when the skin fibroblasts were removed from the culture or replaced with colon stromal cells (Figures 3E and 3F). Consistent with our findings (Figure 1), the expression of mRNA encoding *P2rx7* was accordingly changed (Figure 3G), and BMMCs cocultured with skin fibroblasts did not produce MCP1 and TNF-α upon extracellular ATP stimulation (Figure 3H). Like P2X7 expression, gene expressions of *Mcpt1*, *Mcpt2*, and *Mcpt4* and the production of heparin and chondroitin sulfate induced

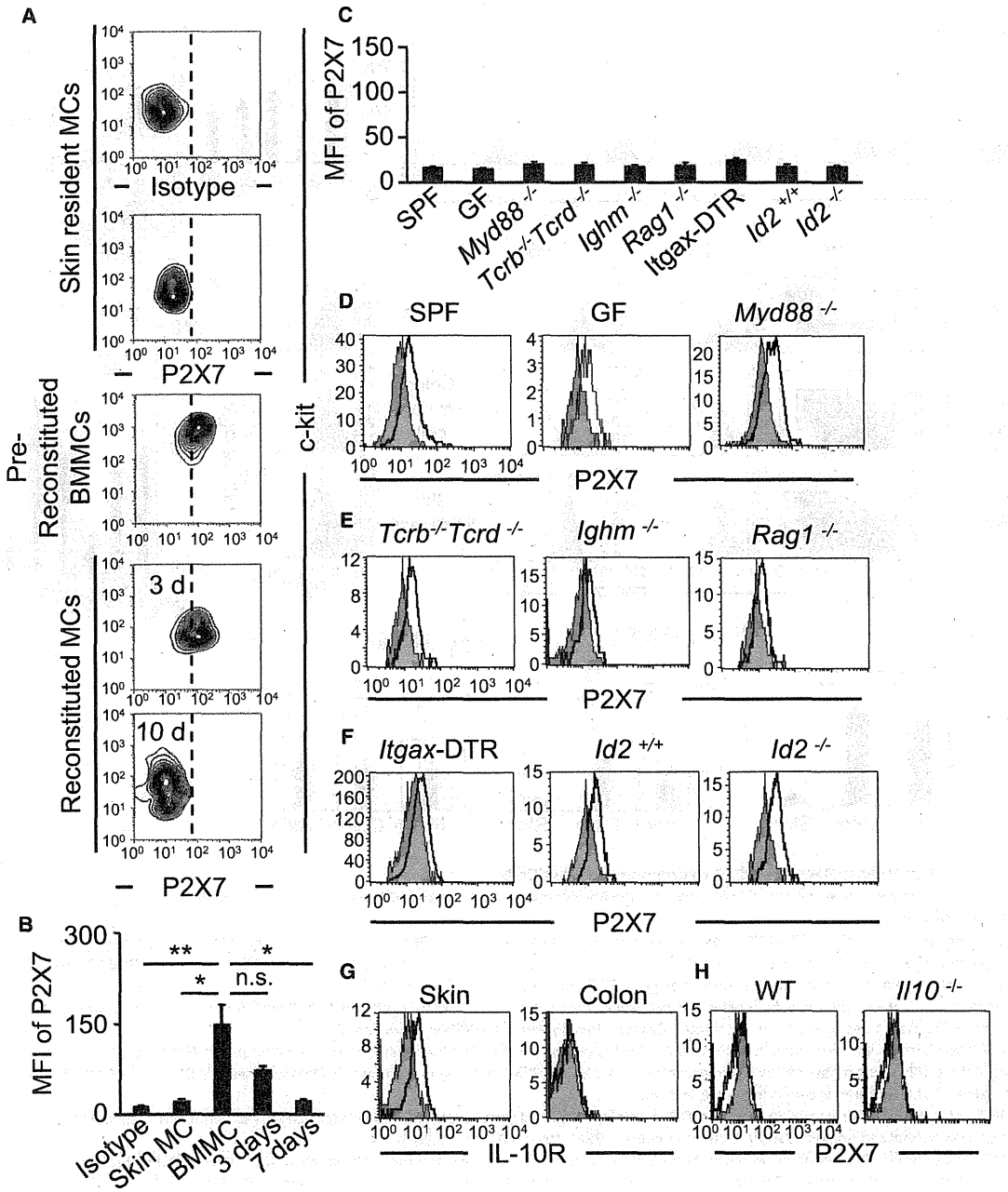

Figure 2. Skin Environment Regulates P2X7 Expression

(A and B) Flow cytometric analysis was performed to measure P2X7 expression on skin MCs from WT or $Kit^{W\text{-}sh/W\text{-}sh}$ mice receiving adaptive transfer of $P2X7^{+}$ bone-marrow-derived MCs (BMMCs) (A) and mean fluorescence intensity (MFI) was examined (B). Data are means ± SEM. *$p < 0.05$ ($n = 3$); **$p < 0.01$; n.s., not significant.

(C–F) MFI of P2X7 expression on skin MCs from various mice were examined by flow cytometry (C). Data are means ± SEM ($n = 3$ to 8). (D-F) P2X7 expression was measured by flow cytometry on skin MCs from specific-pathogen free (SPF), germ free (GF), and $Myd88^{-/-}$ mice (D), and $Tcrb^{-/-}Tcrd^{-/-}$, $Ighm^{-/-}$, and $Rag1^{-/-}$ mice (E), diphtheria-toxin-treated *Itgax*-DTR transgenic, $Id2^{+/+}$, and $Id2^{-/-}$ mice (F). Control staining with isotype control is shown as gray.

(G) IL-10 receptor (IL-10R) expression on MCs from skin and colon was analyzed by flow cytometry.

(H) P2X7 expression on skin MCs was measured in WT and $Il10^{-/-}$ mice. Control staining with isotype control is shown as gray. All data are representative of at least three independent experiments.

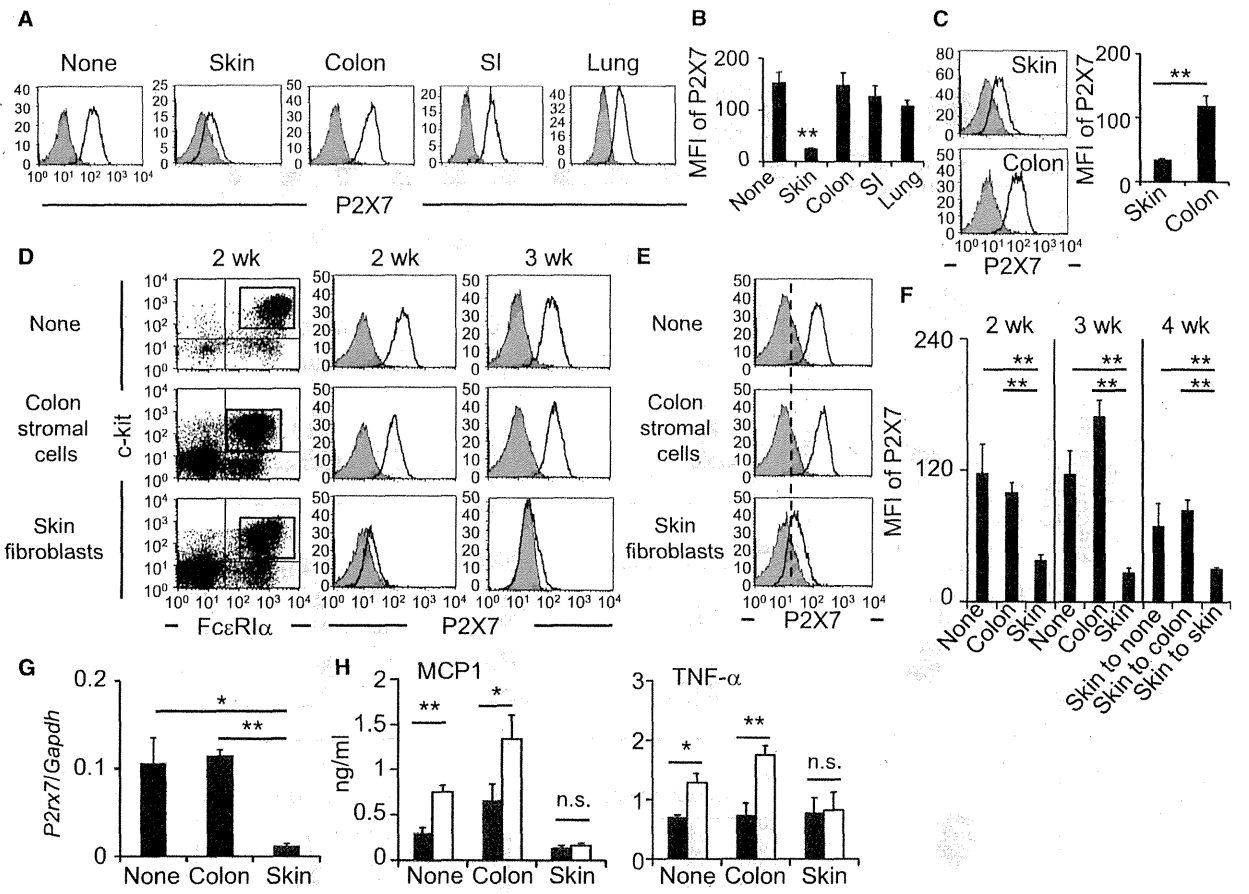

Figure 3. Skin Fibroblasts Regulate P2X7 Expression on Mast Cells

(A) BMMCs were cultured with or without skin fibroblasts, lung fibroblasts, or small intestine (SI) or colon stromal cells and stained for P2X7. Control staining with rat IgG2b is shown as gray.

(B) Mean fluorescence intensity (MFI) of P2X7 expression is shown. Data are means ± SEM. $^{**}p < 0.01$, one-way ANOVA and Tukey's method (n = 5 to 8).

(C) BMMCs and colon stromal cells or skin fibroblasts were separately cultured in the transwells for 3 weeks. P2X7 expression BMMCs was measured by flow cytometry. Control staining with rat IgG2b is shown as gray. Data are means ± SEM (n = 6). $^{**}p < 0.01$.

(D) Bone marrow cells were cultured with or without skin fibroblasts or colon stromal cells, together with IL-3 and stem cell factor for 3 weeks. Expression of c-kit, FcεR1α, and P2X7 was measured by flow cytometry. Control staining with rat IgG2b is shown as gray.

(E and F) Bone-marrow cells were cocultured with skin fibroblasts for 3 weeks and then cultured with or without skin fibroblasts or colon stromal cells for an additional 4 days. P2X7 was measured by flow cytometry (E) and MFI of P2X7 expression is shown (F). Data are means ± SEM. $^{**}p < 0.01$, (n = 4 to 6). All data are representative of at least three independent experiments.

(G) BMMCs were sorted after coculture with skin fibroblasts and colon stromal cells, and *P2rx7* expression was examined by quantitative RT-PCR. Relative expression was normalized against *Gapdh*. Data are means ± SEM. $^{**}p < 0.01$, $^{*}p < 0.05$ (n = 4).

(H) BMMCs were sorted after coculture with skin fibroblasts and colon stromal cells and then stimulated with 0.5 mM ATP. Production of MCP1 and TNF-α in culture supernatant was determined. Black bars, no treatment; white bars, ATP stimulation. Data are means ± SEM. $^{*}p < 0.05$, $^{**}p < 0.01$, n.s. not significant.

by coculture with skin fibroblasts were reversed by removal of skin fibroblasts or replacement with colon stromal cells (Figures S3E and S3F). These results suggest that skin fibroblasts play a pivotal role in the downregulation of P2X7 expression on MCs, leading to the blockade of their reactivity to extracellular ATP.

Cyp26b1 Plays a Critical Role in Negative Regulation of P2X7 Expression on MCs

Gene expression was compared between skin fibroblasts and colon stromal cells, as an example of P2X7-inhibitor and noninhibitor cells, respectively. Gene microarray analysis identified several genes expressed more highly in skin fibroblasts than in colonic stromal cells, including gene encoding the retinoic-acid (RA)-degrading enzymes *Cyp26a1* and *Cyp26b1* (Figure 4A). Quantitative RT-PCR analysis confirmed the higher expression of *Cyp26b1* in the skin fibroblasts than colonic stromal cells (Figure 4B), whereas *vimentin*, a stromal cell pan-marker, was identically expressed in both cell types (Figure 4C). It was reported that Cyp26b1 is involved in skin homeostasis and thus increases in RA concentrations through disruption of *Cyp26b1* cause abnormalities in embryonic skin barrier formation (Okano et al., 2012). In addition, in vitro culture of $CD8^+$ T cells with RA induces

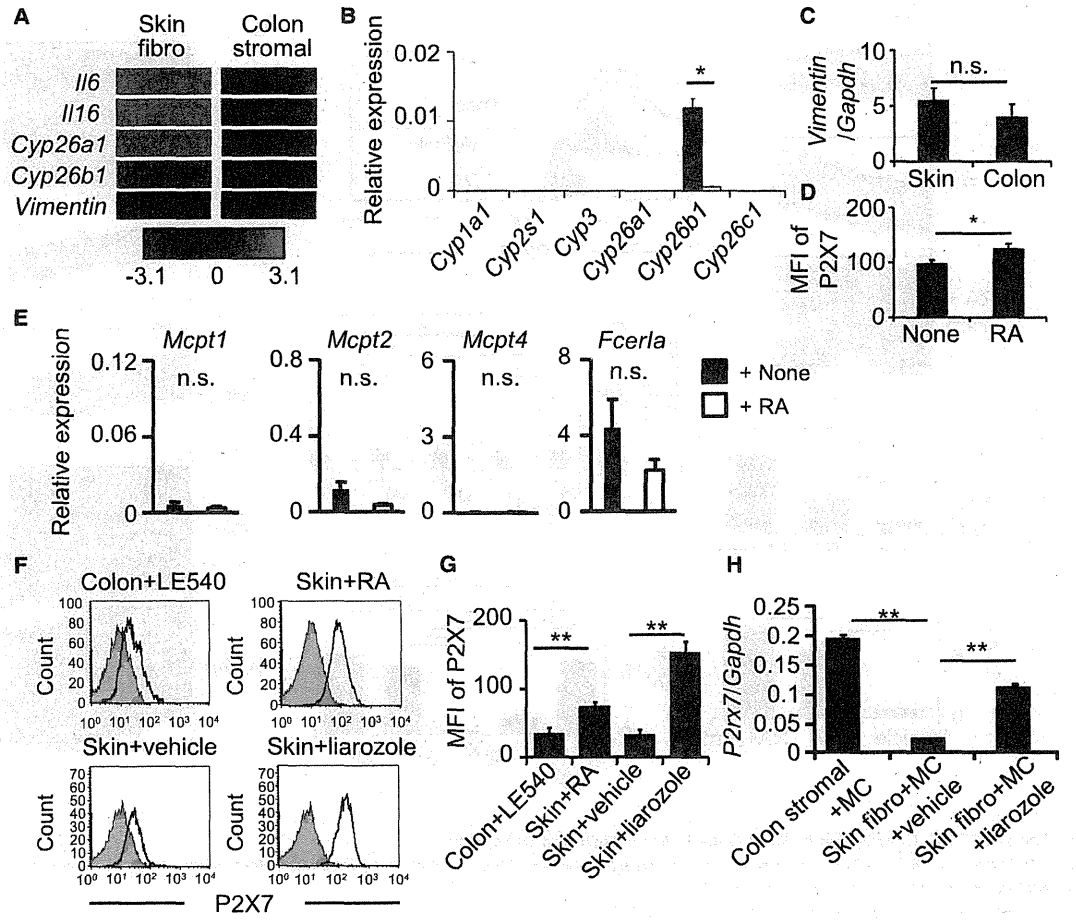

Figure 4. Critical Role of Cyp26b1 in Regulating P2X7 Expression on Mast Cells

(A) Gene microarray analysis was performed to compare the gene expression between skin fibroblasts and colon stromal cells; representative genes are shown.

(B) Gene expression of Cyp26 families was examined by quantitative RT-PCR. Gene expression relative to *Gapdh* is shown. Data are means ± SEM. *$p < 0.05$ ($n = 4$).

(C) Vimentin expression on skin fibroblasts and colon stromal cells was examined by quantitative RT-PCR (qRT-PCR). Relative expressions were normalized against *Gapdh*. Data are means ± SEM ($n = 4$). n.s., not significant.

(D and E) BMMCs were treated with 50 nM of retinoic acid (RA) for 6 days. The expression of P2X7 (D) and *Mcp1*, *Mcp2*, *Mcp4* and *Fcerla* (E) was then examined by flow cytometry and qRT-PCR, respectively. Data are means ± SEM ($n = 4$). *$p < 0.05$.

(F) BMMCs were cocultured with skin fibroblasts or colon stromal cells, with or without RA, LE540, or liarozole and stained for P2X7. Control staining with rat IgG2b is shown as gray. Data are representative of at least three independent experiments.

(G) MFI of P2X7 expression was shown ($n = 3$ to 6). Data are means ± SEM. **$p < 0.01$.

(H) *P2rx7* expression on cocultured BMMCs was examined by qRT-PCR. Data are means ± SEM ($n = 4$). **$p < 0.01$.

P2X7 expression (Heiss et al., 2008). Therefore, it is possible that Cyp26b1-mediated control of RA concentrations by skin fibroblasts regulates P2X7 expression on MCs. To test this hypothesis, we examined the P2X7 expression after adding RA to BMMCs. P2X7 expression increased in the presence of RA without affecting gene expression of *Mcpt1*, *Mcpt2*, and *Mcpt4* (Figures 4D and 4E). Similarly, adding RA to BMMCs in the presence of skin fibroblasts also increased the P2X7 expression (Figures 4F and 4G). Reciprocally, LE540, an inhibitor of retinoid X receptor and retinoid A receptor, suppressed the P2X7 expression on MCs cocultured with colon stromal cells (Figures 4F and 4G). In addition, in vitro treatment of skin fibroblasts with liarozole, a Cyp26b1 inhibitor, augmented P2X7 expression on MCs (Figures 4F–4H). These data demonstrate the critical roles of skin fibroblasts in modulation of P2X7 expression on MCs via the RA metabolic enzyme Cyp26b1.

Aberrant P2X7 Expression on MCs Induces Skin Inflammation, and Its Inhibition Ameliorates Disease Development

Retinoid and its metabolites play important roles in both pro- and anti-inflammatory responses (Fisher and Voorhees, 1996). Retinoids display key physiological roles in maintaining skin homeostasis, and dysregulation of retinoid signaling is found in various skin diseases. Indeed, topical treatment with retinoids causes epidermal hyperplasia and thickening of the differentiated

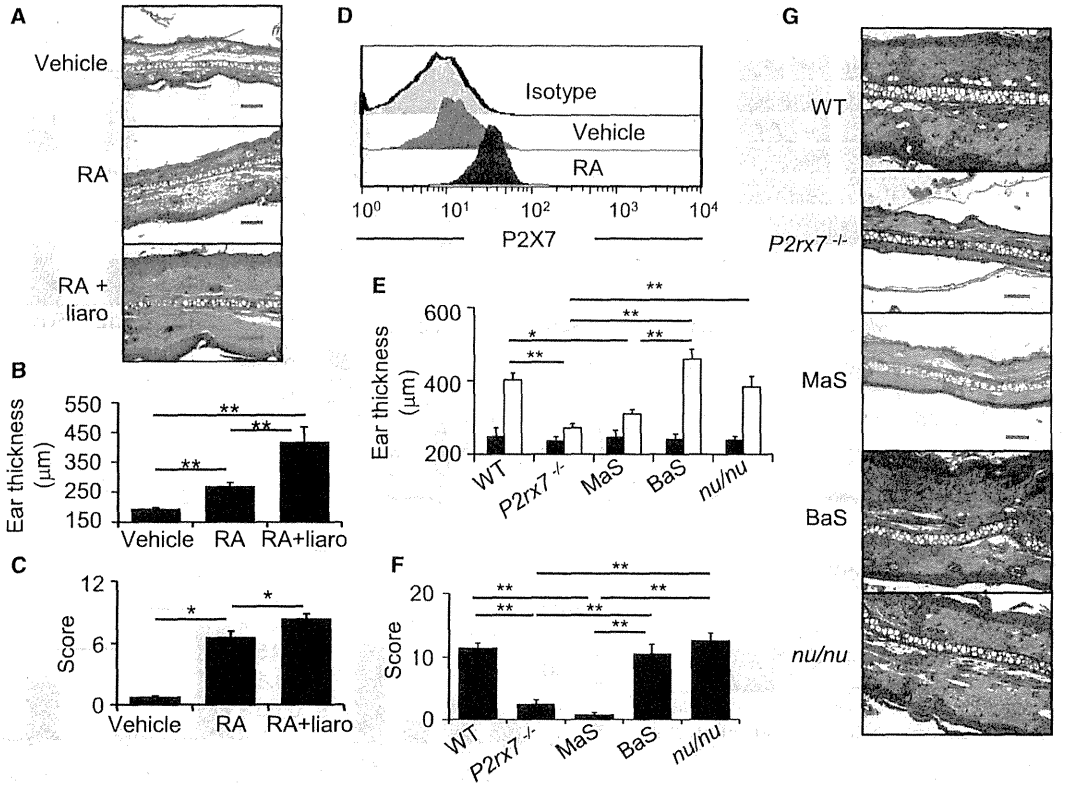

Figure 5. Aberrant P2X7 Expression in Mast Cells Induces Retinoid Dermatitis

(A) Hematoxylin and eosin (H&E) staining of skin from mice treated with vehicle or RA with or without liarozole (liaro) for 2 weeks. Data are representative of at least three independent experiments. Scale bars represent 100 μm.

(B) Thickness of ear was measured. Data are means ± SEM. $^{**}p < 0.01$ (n = 4).

(C) Severity of inflammation was scored. Data are means ± SEM. $^{*}p < 0.05$ (n = 4).

(D) Expression of P2X7 on skin MCs in RA- or vehicle-treated mice was examined by flow cytometry analysis.

(E) Mice (WT; diphtheria toxin-treated MaS-TRECK, MaS; diphtheria toxin-treated BaS-TECK, BaS; and nude; *nu/nu*) were treated with RA for 8 weeks and ear thickness was measured (n = 6 to 24).

(F) Severity of inflammation was scored (n = 3 to 4) (means ± SEM. $^{*}p < 0.05$, $^{**}p < 0.01$, one-way ANOVA and Tukey's method).

(G) Representative H&E staining of ear are shown. Scale bars represent 100 μm.

suprabasal layers, eventually leading to retinoid dermatitis (Fisher and Voorhees, 1996; García-Serrano et al., 2011). Additionally, skin irritation occurs with retinoid treatment (Varani et al., 2003). High-dose oral administration of RA to pregnant mice causes skin inflammation in the fetus (Okano et al., 2012). These findings led to a hypothesis that P2X7 expression on skin MCs induced by high concentration of RA might be of relevance to skin irritation or retinoid dermatitis.

To test this hypothesis, mice were orally inoculated with 0.4% RA twice a week for several weeks. These RA-treated mice showed skin irritation and hypertrophy when compared with vehicle-treated mice (Figures 5A–5C; Figure S4A). Histological analysis showed that RA treatment caused dermatitis associated with the accumulation of inflammatory cells and MCs (Figures 5A; Figure S4B–S4E). Importantly, P2X7 expression in skin MCs in RA-treated mice was augmented compared with that in vehicle-treated mice (Figure 5D). Moreover, inhibition of Cyp26b1-dependent RA metabolism by the treatment with liarozole exacerbated the skin inflammation compared with RA treatment alone (Figures 5A–5C; Figure S4B). These results indicated that Cyp26b1 counteract the onset of RA-induced dermatitis. Furthermore, RA-induced dermatitis was ameliorated in *P2rx7*$^{-/-}$- and MC-deficient mice, but not in basophil-deficient mice (Figures 5E–5G).

We confirmed a previous report (Hall et al., 2011) that RA induces the differentiation of both T helper 17 (Th17) and regulatory T cells (Figure S4F). RA treatment also slightly induced P2X7 expression on skin T cells (Figure S4G). Therefore, to evaluate the possible involvement of T cells in the induction of RA-induced dermatitis, we analyzed T cell-deficient nude (*nu/nu*) mice (Figures 5E–5G). We observed ear swelling accompanied by inflammation in *nu/nu* mice (Figures 5E–5G), indicating that, even though RA treatment affected the P2X7 expression in both T cells and MCs, MCs play central roles in the induction of retinoid dermatitis.

To examine the expression of P2X7 ligands in retinoid dermatitis, we next measured the production of extracellular ATP—a major ligand of P2X7—in mice with retinoid dermatitis or mice receiving skin scratch as a control (Kawamura et al., 2012). We detected elevated amounts of ATP in the skin of mice with

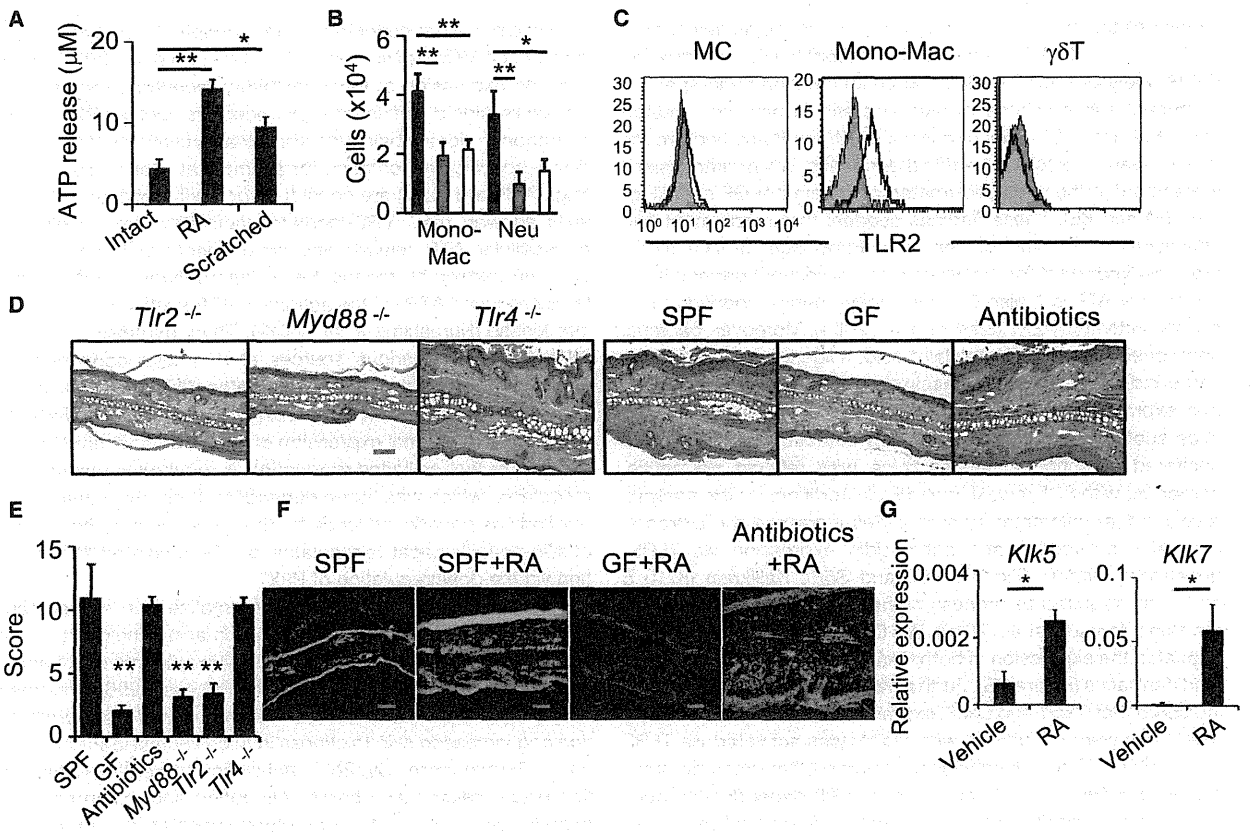

Figure 6. Skin Commensal Bacteria Contribute to P2X7-Medaited Retinoid Dermatitis

(A) ATP concentrations released from skin tissues were measured (means ± SEM. *$p < 0.05$; **$p < 0.01$).

(B) The numbers of monocytes and macrophages (Mono-Mac) and neutrophils (Neu) in the skin after RA-treatment were quantified (black bars, WT; gray bars; *P2x7*$^{-/-}$; white bars, diphtheria toxin-treated MaS-TRECK mice) (means ± SEM. *$p < 0.05$; **$p < 0.01$).

(C) TLR2 expression was examined in MCs, CD11b^{+} Mono-Mac, and γδ T cells. Control staining with isotype control antibody is shown as gray.

(D) *Tlr2*$^{-/-}$, *Myd88*$^{-/-}$, and *Tlr4*$^{-/-}$, specific-pathogen-free (SPF), germ-free (GF), and antibiotic-treated mice were treated with retinoic acid for 8 weeks; representative hematoxylin and eosin staining of ear are shown. Data are representative of at least three independent experiments. Scale bars represent 100 μm.

(E) Severity of inflammation was scored ($n = 4$ to 6). Data are means ± SEM. **$p < 0.01$; one-way ANOVA and Tukey's method.

(F) Cathelicidin (green) expression was measured by confocal microscopy. Scale bars represent 100 μm.

(G) Kallikrein (KLK) 5 ($n = 9$) and 7 ($n = 4$) expression was examined by qRT-PCR. Data are means ± SEM. *$p < 0.05$.

retinoid dermatitis as scratched skin (Figure 6A). In addition, degradation of extracellular ATP by local administration of apyrase suppressed at least partly the severity of retinoid dermatitis (Figures S5A–S5C). The ATP-P2X7 pathway leads to the production of lipid mediators (e.g., leukotriene B4) and chemokines (e.g., MCP1, CCL7, and CXCL2) from MCs to recruit inflammatory cells such as monocytes and neutrophils (Kurashima et al., 2012). We found that CD11b^{+} monocytes and macrophages and Gr-1^{+} neutrophils were increased in the skin of mice treated with RA, but their abundance was lower in RA-treated mice lacking P2X7 or MCs (Figure 6B). These results suggest that increased ATP production in the RA-treated skin caused P2X7- and MC-dependent skin inflammation.

P2X7-Mediated Retinoid Dermatitis Requires Innate Immune Signaling

External stimuli—especially antimicrobial signaling—can provoke or inhibit skin inflammation (Jin et al., 2009). We found that TLR2 was highly expressed by the accumulated cells (e.g., monocytes and macrophages) but relatively low in MCs and γδ T cells (Figure 6C). To determine whether microbial stimulation via TLR2 participated in the induction of retinoid dermatitis, *Tlr2*$^{-/-}$ and *Myd88*$^{-/-}$ mice were inoculated with a high dose of RA. Those mice had only minor incidence of retinoid dermatitis after 8 weeks of RA inoculation, whereas identically treated *Tlr4*$^{-/-}$ mice had typical signs of retinoid dermatitis (Figures 6D and 6E). These results suggest that signaling from TLR2 contributes to the development of retinoid dermatitis. It remains unclear whether TLR2 signaling is mediated by microbial components, because other endogenous ligands, such as hyaluronan fragments, biglycan, and serum amyloid A, also activate TLR2 (Erridge, 2010). Therefore, to determine the requirement for TLR2 ligands derived from skin microbiota, we induced retinoid dermatitis in GF mice. In addition, we used mice receiving antibiotics orally because, unlike GF mice, which were free from both gut and skin microbiota, oral antibiotic administration rarely

influences the skin microbiota but diminishes the gut microbiota (Naik et al., 2012). Whole-mount fluorescent in situ hybridization (FISH) analysis with EUB338 (a probe for most bacterial species) confirmed the presence of skin bacteria in antibiotic-treated mice, but not in GF mice (Figure S5D). When these two groups of mice were subjected to retinoid dermatitis, inflammatory signs were found in the antibiotic-treated mice, but not GF mice (Figures 6D and 6E). These findings suggest that recruitment and activation of $TLR2^+$ monocytes and macrophages by skin microbiota are important for the aggravation of retinoid dermatitis.

Not only ATP but also the cathelicidin-derived peptide LL37 directly activates P2X7 (Elssner et al., 2004). Moreover, bacterial components such as lipoteichoic acid, a ligand of TLR2, induce cathelicidin production (Yamasaki et al., 2007). Indeed, we found that expression of gene encoding *cathelicidin* were low in GF mice subjected to retinoid dermatitis induction, but they were unaltered in antibiotic-treated mice with retinoid dermatitis, compared with SPF mice (Figure 6F). In addition, in vitro analysis revealed that inflammatory monocytes increased the extracellular ATP production and cathelicidin expression via TLR2-dependent manner (Figures S5E and S5F). Kallikrein (KLK) 5 and 7 are required to process cathelicidin to produce LL37 in the skin (Morizane et al., 2010). We found that RA treatment upregulated the expression of both *Klk5* and *Klk7* in the area of retinoid dermatitis (Figure 6G). Furthermore, another in vitro analysis indicated that *Cxcl1* and *Cxcl2* expression was increased in MCs when they were cocultured with monocytes activated via TLR2 (Figure S5G). These observations indicated that cross-communication between skin microbiota- and TLR2-dependent production of P2X7 ligands such as ATP and LL37 from inflammatory monocytes and the activation of MCs via P2X7 is critical for the development of retinoid dermatitis.

DISCUSSION

Skin and mucosa possesses immunologically unique regulatory systems that create balanced homeostatic conditions in the face of the harsh outside environment. It was suggested that tissue environmental factors regulate locally unique MC phenotypes (Xing et al., 2011). As protease expression patterns on MCs (Xing et al., 2011), our previous findings suggested that P2X7 expression on MCs differs between the skin and intestine (Kurashima et al., 2012). Here, we found a function of skin fibroblasts in reducing the P2X7 expression on MCs through the metabolism of RA. This pathway creates unique niches for regulating the homeostatic network of the skin-surface barrier by inhibiting excessive ATP-mediated activation of MCs. We also proposed the possible involvement of LL37 as another ligand of P2X7 in skin inflammation. These observations reveal the unique tissue-dependent immune regulation mediated by structural cells such as stromal cells and fibroblasts to create homeostasis at the skin-surface barrier. Breakdown of this system leads to the development of inflammation such as retinoid dermatitis.

Activation of MCs is tightly regulated by multiple receptors. For instance, elevated expression of IL-33 from epidermal keratinocytes and dermal fibroblasts as a result of sun exposure induces MC activation and hence skin inflammation (Lunderius-Andersson et al., 2012). Simultaneously, various inhibitory receptors, such as leukocyte monoimmunoglobulin-like receptor 3 and paired immunoglobulin-like receptor B, are typically expressed on MCs (Izawa et al., 2012; Masuda et al., 2007). Along with the expression of these inhibitory receptors, regulation of the expression of activation-type receptors such as P2X7 might be important for inhibiting the abnormal activation of MCs under tissue-specific environment, for example at sites where ligands (e.g., ATP and LL37) are constantly or easily produced. Our results showed that TLR2-mediated activation was involved in extracellular ATP release and simultaneous enhancement of LL37 production by monocytes or macrophages. Furthermore, MCs produced ATP via the actions of ATP synthase and adenylate kinase (Kurashima et al., 2012). Thus, extracellular ATP is released from a various sources at millimolar concentration, which are sufficient for P2X7-mediated MC activation at the site of skin inflammation (Takahashi et al., 2013). Therefore, the balanced and optimal expression of activation and inhibitory receptors, as well as ligand production, is required to maintain homeostasis, which was tissue dependent. From this perspective, our findings provide evidence for the presence and mechanism of skin-specific negative regulation of ATP-mediated MC activation via the downregulation of P2X7.

RA has been used clinically to normalize skin homeostasis in patients with acne or psoriasis (Geria and Scheinfeld, 2008). However, topical application of excessive amounts of RA accelerates skin inflammation (Fisher and Voorhees, 1996). Treatment with excessive amounts of 9-*cis* RA causes epidermal proliferation and increased skin thickness in mice (García-Serrano et al., 2011). Furthermore, Cyp26b1 deficiency in keratinocytes and fibroblasts causes skin barrier disruption and inflammation in mice (Okano et al., 2012). Our study indicated the importance of RA-mediated upregulation of P2X7 on MCs in the development of skin inflammation. Liarozole inhibits RA metabolism with targeting not only Cyp26b1 but other P450 enzymes; thus, off-target effects of liarozole could not be negligible (De Coster et al., 1996). Our data indicated the highest expression of Cyp26b1 in skin fibroblasts; these data, plus those from the studies mentioned above, reflect the important aspects and kinetics of the skin fibroblast-Cyp26b1-mediated regulatory and inhibitory system for creating and maintaining a physiologically optimized skin-surface barrier system.

Mcpt expression is reversibly regulated by the tissue environment (Xing et al., 2011). Our data indicate that RA does not regulate Mcpt expression, suggesting that the soluble signals emanating from stromal cells and fibroblasts for MC differentiation and for downregulation of P2X7 expressions differ from each other. Our current findings also revealed that coculture with lung fibroblasts partially reduced P2X7 expression in BMMCs. This effect on P2X7 expression was weaker than that of skin fibroblasts; moreover, P2X7 suppressive capacity was correlated with reduced expression of Cyp26b1 (data not shown). Because concentrations of extracellular ATP were high in respiratory inflammation and lung MCs in vivo expressed high P2X7 (Idzko et al., 2007), reducing P2X7 expression on MCs by enhancing Cyp26b1 expression in fibroblasts in the lung would be a therapeutic strategy for respiratory disorders.

MCs are involved in various skin inflammation, such as psoriasis, atopic dermatitis, and alopecia areata (Cetin et al., 2009; Gilfillan and Beaven, 2011; Otsuka et al., 2011). In this context, high vitamin A concentration in serum is associated with a risk

of atopic dermatitis (Kull et al., 2006). In addition, it was recently reported that dietary vitamin A is involved in aggravating chronic inflammatory status in alopecia both in mice and human (Duncan et al., 2013). In mice with alopecia areata, RA synthesis is increased and simultaneously RA degradation is decreased, thus resulting in excess concentrations of RA at the site of skin inflammation (Duncan et al., 2013). Indeed, P2X7$^+$ MCs are accumulated at the site of alopecia in human (data not shown). These results imply that dysregulation of P2X7 expression on MCs occurs in particular skin inflammation associated with disruption and interruption of RA metabolism. Therefore, it is possible that RA-induced P2X7–MC cascades are also involved in the RA-related skin inflammation.

Skin-resident bacteria play an autonomous role in controlling the local inflammatory milieu by modulating the function of skin-resident T cells (Naik et al., 2012). Functional TLRs are expressed on MCs (Matsushima et al., 2004; Sandig and Bulfone-Paus, 2012). In addition, cathelicidin expression on MCs is induced by the activation of TLR2 by lipoteichoic acid produced by commensal bacteria. Indeed, TLR2 is highly expressed on BMMCs (Wang et al., 2012). Therefore, it is possible that P2X7 and TLR2 dual pathways affect the skin MC-induced production of inflammatory mediators. However, our experiments with three different clones (6C2, mT2.7, and mT2.5) of anti-TLR2 monoclonal antibodies revealed that TLR2 was poorly expressed on the surfaces of skin MCs. Indeed, reconstitution of TLR2-deficient MCs to the MC-deficient mice showed retinoid dermatitis after RA-treatment (data not shown). In contrast, CD11b$^+$ monocytes and macrophages in the skin highly expressed TLR2, indicating that skin-microbiota-mediated signaling stimulates accumulation and activation of inflammatory cells in the skin; this might initiate disruption of skin homeostasis, including the skin fibroblast-Cyp26b1-mediated downregulation system of P2X7-dependent MC activation. In addition, recruitment or activation of the TLR2-expressing inflammatory cells is led by chemokines (e.g., MCP1) or lipid mediators (e.g., leukotrienes) released upon MC activation and the induction of inflammatory responses by ATP release. MCs also directly regulate DC activation in the skin; indeed, maturation and migration of DCs are regulated by TNF-α and ICAM1 on MCs; thus, MC-DC direct interaction could also affect the pathogenesis of skin inflammation (Otsuka et al., 2011). Our in vitro observation revealed that TLR2$^+$ inflammatory cells directly enhanced CXCL1 and CXCL2 expression in MCs, which potentially led to the neutrophil recruitment into the inflammatory site. These results implied the existence of the inflammatory loop among various immune cells including MCs.

These findings collectively reveal that MCs in various tissues help to create tissue-specific local homeostasis operated by individual structural cells (e.g., fibroblasts). Cyp26b1-expressing skin fibroblasts thus play a central role in homeostatic P2X7 downregulation on skin MCs, leading to the suppression of ATP-induced abnormal activation. When the skin homeostatic pathway is sporadically interrupted, such as in hypervitaminosis A, skin bacterial stimulation triggers inflammation via the TLR2-mediated pathway. Our additional understanding of the molecular and cellular bases of the functions and phenotypes of localized MCs and their surrounding structural cells (e.g., fibroblasts and stromal cells) will facilitate the discovery of innovative and beneficial targets for the control of tissue-specific inflammation.

EXPERIMENTAL PROCEDURES

Mice

C57BL/6, Balb/c, GF, and *nu/nu*$^{-/-}$ mice were purchased from Japan CLEA. *Rag1*$^{-/-}$, *Tcrb*$^{-/-}$, *Tcrd*$^{-/-}$, *Ighm*$^{-/-}$, *P2rx7*$^{-/-}$, and *Itgax*-DTR mice were obtained from Jackson Laboratory. *Tlr2*$^{-/-}$, *Tlr4*$^{-/-}$, and *Myd88*$^{-/-}$ mice were obtained from Dr. S. Akira (Osaka University). *Id2*$^{-/-}$ mice were generated as previously described (Yokota et al., 1999). *Kit*$^{W\text{-}sh/W\text{-}sh}$ mice were obtained from Dr. H. Suto (Juntendo University). MaS-TRECK and BaS-TRECK mice were established as previously reported (Sawaguchi et al., 2012). All mice were maintained under SPF or GF conditions at the Experimental Animal Facility of the Institute of Medical Science, the University of Tokyo. All experiments were approved by the Animal Care and Use Committee of the University of Tokyo.

In Vivo Treatment

To remove DCs, we intraperitoneally treated *Itgax*-DTR mice with DT (500 ng, Sigma-Aldrich) (Jung et al., 2002). To deplete MCs and basophils, we injected MaS-TRECK and BaS-TRECK mice intraperitoneally with 250 ng DT for 5 consecutive days and then with 150 ng DT every other day (Sawaguchi et al., 2012). Mice were orally inoculated with 0.4% RA (Sigma-Aldrich) in corn oil (Wako) twice a week. Liarozole (1 mg, intraperitoneally) or apyrase (1U/ear, grade VII, Sigma-Aldrich, intradermally) was injected before RA treatment. Mice received a mixture of ampicillin (1 g/L; Sigma-Aldrich), vancomycin (500 mg/L; Shionogi), neomycin (1 g/L; Sigma-Aldrich), and metronidazole (1 g/ L; Sigma-Aldrich) in drinking water since 2 weeks before RA treatment (Obata et al., 2010). MCs were reconstituted in *Kit*$^{W\text{-}sh/W\text{-}sh}$ mice by intraperitoneal and intravenous (5×10^6 cells each) or intradermal (1×10^6 cells) injection of BMMCs.

Cell Preparations

Mononuclear cells from the small intestine, colon, PEC, lung, and skin were isolated, and BMMCs were obtained as previously described (Kurashima et al., 2012; Kurashima et al., 2007). To prepare stromal cells and fibroblasts, tissues were digested with EDTA and collagenase (Sigma-Aldrich) and adherent cells were passaged every 4 days (process repeated once). Before coculture with BMMCs, cells were treated with 10 ng/ml mitomycin C (Sigma-Aldrich) for 3 hr and washed twice with PBS. In some experiments, BMMCs were cytospinned (600 rpm, 4 min) and stained for 1 hr with alcian blue (Muto Pure Chemicals, Tokyo, Japan) and for 20 min with safranin (Muto Pure Chemicals). Inflammatory monocytes or macrophages were collected from PEC 3 days after intraperitoneal injection of 2 ml of 4% thioglycolate.

In Vitro Treatment

For MCP1 and TNF-α measurement, 2×10^5 cells were stimulated with 0.5 mM of ATP for 2 days. For IL-1β measurement, 2×10^5 cells were stimulated with 0.1 μg/mL LPS for 8 hr, followed by 0, 0.5, or 5 mM of ATP for 1 hr. Chemokine and cytokine production in the culture supernatant was measured with CBA inflammatory cytokine kit (BD Biosciences) and IL-1β ELISA (R&D Systems). To stimulate TLR2-mediated pathway, we cultured thioglycolate-induced monocytes and macrophages with Pam2CSK4 (0.2 μg/mL, InvivoGen). To measure ATP secretion from skin organ, we floated skin (8.0 mm square) with the epidermis side upward on 12-well plates containing 1 ml PBS and incubated on ice for 10 min. ATP concentration in the culture was measured by ATP luciferase assay (PerkinElmer) (Kawamura et al., 2012; Kurashima et al., 2012).

Flow Cytometry

Cells were incubated with 5 μg/ml of anti-CD16/32 antibody (Biolegend) for 5 min and then stained for 30 min at 4°C with fluorescence-labeled antibodies; c-kit (0.2 μg/mL), Gr-1 (0.4 μg/mL), CD4 (1 μg/mL), CD11b (0.2 μg/mL), CD11c (0.4 μg/mL), and B220 (0.4 μg/mL) (BD Biosciences); FcεRIα (0.4 μg/mL) and CD207 (0.4 μg/mL) (eBioscience); and F4/80 (20 μg/mL) and ER-TR7 (5 μg/mL) (Abcam), and P2X7 (2 μg/mL, clone 1F11) (Kurashima et al., 2012). Flow cytometric analysis and cell sorting were performed with FACSCalibur and FACSAria (BD Biosciences), respectively.

Histology and Scoring

Skin samples were fixed in 4% paraformaldehyde and embedded in paraffin. Tissue sections (5 μm) were stained with hematoxylin and eosin (Wako). To

stain collagen$^+$ fibroblasts, we stained tissue sections with anilin blue orange G solution (Muto Pure Chemicals) for 1 hr and counterstained with toluidine blue (Wako) for 20 min. For the staining with anti-mouse cathelicidin antibody (Abcam), tissue sections were retrieved with Retrievagen A (BD Biosciences).

Inflammation severity was scored as follows: 0, no; 1, minimal; 2, mild; 3, moderate; and 4, marked. The slides were blinded, randomized, and reread to determine score. The total score was calculated as the sum of scores for inflammation, neutrophil number, mononuclear cell number, edema, and epithelial hyperplasia (Otsuka et al., 2011).

Whole-Mount FISH

Skin was fixed in 4% paraformaldehyde at 4°C overnight and washed with PBS for 7 hr. Tissues were hybridized with 10 μg/mL of Alexa 488-conjugated DNA probe (EUB338, Invitrogen) in a hybridization buffer (0.9 M NaCl, 20 mM Tris-HCl, 0.1% SDS, and 10 μg/mL) at 42°C overnight. After washing twice in a washing buffer (0.45 M NaCl, 20 mM Tris-HCl, 0.01% SDS) at 42°C for 10 min, tissues were flushed with PBS and observed by confocal microscopy (DM IRE2/TCS SP2, Leica) (Obata et al., 2010).

Microarray Analysis

Total RNA was prepared with RNeasy kit (QIAGEN). cRNA was hybridized with DNA probes on a GeneChip Mouse Genome 430 2.0 array (Affymetrix) (Kunisawa et al., 2013). Data were analyzed with GeneSpring 7.3.1 software (Silicon Genetics).

Quantitative RT-PCR

Total RNA was prepared with TRIzol (Invitrogen) and reverse transcribed by Superscript VILO (Invitrogen). Quantitative RT-PCR was performed with the LightCycler 480 II (Roche) and the Universal Probe Library (Roche). Primer sequence is available in Table S1.

Statistical Analysis

Statistical analysis was performed with the unpaired two-tailed Student's t test and Welch's t test. In some experiments, one-way ANOVA and Tukey's method were employed as indicated in figure legends.

SUPPLEMENTAL INFORMATION

Supplemental Information includes one table and five figures and can be found with this article online at http://dx.doi.org/10.1016/j.immuni.2014.01.014.

AUTHOR CONTRIBUTIONS

Y. Kurashima conducted the research, performed experiments, and wrote the manuscript. T.A., K.F., Y. Kogure, Y.S., and E.H. performed gene expression and animal experiments. N.S. conducted in situ experiments. K.K. and A.O. contributed to the experimental design, skin analysis, and histological scoring. M.K., S.A., and S.S. helped construct the transgenic mice. T.S. conducted the morphological analysis of MCs. K.M., J.K., and H.K. supervised the project and wrote the manuscript.

ACKNOWLEDGMENTS

We thank H. Suto (Atopy Research Center, Juntendo University, Tokyo) for providing *Kit*$^{W\text{-}sh/W\text{-}sh}$ mice, and S. Nakae (University of Tokyo) for advice on analyzing *Kit*$^{W\text{-}sh/W\text{-}sh}$ mice. We also thank Y. Yokota (School of Medicine, University of Fukui, Fukui) for providing *Id2*$^{-/-}$ mice. This work was supported by grants from the Ministry of Education, Science, Sports, and Technology of Japan (Grant-in Aid for Scientific Research S [H.K.] for Scientific Research on Innovative Areas [J.K.]; grant from the Leading-edge Research Infrastructure Program [to J.K., H.K.]); from the Young Researcher Overseas Visits Program for Vitalizing Brain Circulation (Japan Society for the Promotion of Science, J.K., H.K., Y.K.); for Japan Society for the Promotion of Science Fellows (Y.K., T.A., N.S.); from the Ministry of Health and Welfare of Japan (J.K., H.K.); from the Global Center of Excellence Program of the Center of Education and Research for Advanced Genome-based Medicine (H.K.); from the Program for Promotion of Basic and Applied Research for Innovations in Bio-oriented Industry (to J.K.); and Kowa Life Science Foundation (J.K.); Kishimoto Foundation Research Grant (J.K.); and from the Yakult Bioscience Foundation (J.K.).

Received: June 25, 2013
Accepted: January 15, 2014
Published: April 10, 2014

REFERENCES

Biggs, L., Yu, C., Fedoric, B., Lopez, A.F., Galli, S.J., and Grimbaldeston, M.A. (2010). Evidence that vitamin D(3) promotes mast cell-dependent reduction of chronic UVB-induced skin pathology in mice. J. Exp. Med. *207*, 455–463.

Cetin, E.D., Savk, E., Uslu, M., Eskin, M., and Karul, A. (2009). Investigation of the inflammatory mechanisms in alopecia areata. Am. J. Dermatopathol. *31*, 53–60.

De Coster, R., Wouters, W., and Bruynseels, J. (1996). P450-dependent enzymes as targets for prostate cancer therapy. J. Steroid Biochem. Mol. Biol. *56* (1-6 Spec No), 133–143.

Di Meglio, P., Perera, G.K., and Nestle, F.O. (2011). The multitasking organ: recent insights into skin immune function. Immunity *35*, 857–869.

Di Virgilio, F. (2007). Liaisons dangereuses: P2X$_7$ and the inflammasome. Trends Pharmacol. Sci. *28*, 465–472.

Duncan, F.J., Silva, K.A., Johnson, C.J., King, B.L., Szatkiewicz, J.P., Kamdar, S.P., Ong, D.E., Napoli, J.L., Wang, J., King, L.E., Jr., et al. (2013). Endogenous retinoids in the pathogenesis of alopecia areata. J. Invest. Dermatol. *133*, 334–343.

Elssner, A., Duncan, M., Gavrilin, M., and Wewers, M.D. (2004). A novel P2X7 receptor activator, the human cathelicidin-derived peptide LL37, induces IL-1 beta processing and release. J. Immunol. *172*, 4987–4994.

Erridge, C. (2010). Endogenous ligands of TLR2 and TLR4: agonists or assistants? J. Leukoc. Biol. *87*, 989–999.

Feyerabend, T.B., Weiser, A., Tietz, A., Stassen, M., Harris, N., Kopf, M., Radermacher, P., Möller, P., Benoist, C., Mathis, D., et al. (2011). Cre-mediated cell ablation contests mast cell contribution in models of antibody- and T cell-mediated autoimmunity. Immunity *35*, 832–844.

Fisher, G.J., and Voorhees, J.J. (1996). Molecular mechanisms of retinoid actions in skin. FASEB J. *10*, 1002–1013.

García-Serrano, L., Gomez-Ferrería, M.A., Contreras-Jurado, C., Segrelles, C., Paramio, J.M., and Aranda, A. (2011). The thyroid hormone receptors modulate the skin response to retinoids. PLoS ONE *6*, e23825.

Geria, A.N., and Scheinfeld, N.S. (2008). Talarozole, a selective inhibitor of P450-mediated all-trans retinoic acid for the treatment of psoriasis and acne. Curr. Opin. Investig. Drugs *9*, 1228–1237.

Gilfillan, A.M., and Beaven, M.A. (2011). Regulation of mast cell responses in health and disease. Crit. Rev. Immunol. *31*, 475–529.

Gurish, M.F., and Austen, K.F. (2012). Developmental origin and functional specialization of mast cell subsets. Immunity *37*, 25–33.

Hacker, C., Kirsch, R.D., Ju, X.S., Hieronymus, T., Gust, T.C., Kuhl, C., Jorgas, T., Kurz, S.M., Rose-John, S., Yokota, Y., and Zenke, M. (2003). Transcriptional profiling identifies Id2 function in dendritic cell development. Nat. Immunol. *4*, 380–386.

Hall, J.A., Grainger, J.R., Spencer, S.P., and Belkaid, Y. (2011). The role of retinoic acid in tolerance and immunity. Immunity *35*, 13–22.

Heiss, K., Jänner, N., Mähnss, B., Schumacher, V., Koch-Nolte, F., Haag, F., and Mittrücker, H.W. (2008). High sensitivity of intestinal CD8$^+$ T cells to nucleotides indicates P2X7 as a regulator for intestinal T cell responses. J. Immunol. *181*, 3861–3869.

Idzko, M., Hammad, H., van Nimwegen, M., Kool, M., Willart, M.A., Muskens, F., Hoogsteden, H.C., Luttmann, W., Ferrari, D., Di Virgilio, F., et al. (2007). Extracellular ATP triggers and maintains asthmatic airway inflammation by activating dendritic cells. Nat. Med. *13*, 913–919.

Izawa, K., Yamanishi, Y., Maehara, A., Takahashi, M., Isobe, M., Ito, S., Kaitani, A., Matsukawa, T., Matsuoka, T., Nakahara, F., et al. (2012). The receptor LMIR3 negatively regulates mast cell activation and allergic responses by binding to extracellular ceramide. Immunity *37*, 827–839.

Jin, H., Kumar, L., Mathias, C., Zurakowski, D., Oettgen, H., Gorelik, L., and Geha, R. (2009). Toll-like receptor 2 is important for the T(H)1 response to cutaneous sensitization. J Allergy Clin Immunol *123*, 875–882, e871.

Jung, S., Unutmaz, D., Wong, P., Sano, G., De los Santos, K., Sparwasser, T., Wu, S., Vuthoori, S., Ko, K., Zavala, F., et al. (2002). In vivo depletion of CD11c+ dendritic cells abrogates priming of $CD8^+$ T cells by exogenous cell-associated antigens. Immunity *17*, 211–220.

Junger, W.G. (2011). Immune cell regulation by autocrine purinergic signalling. Nat. Rev. Immunol. *11*, 201–212.

Kawamura, T., Ogawa, Y., Nakamura, Y., Nakamizo, S., Ohta, Y., Nakano, H., Kabashima, K., Katayama, I., Koizumi, S., Kodama, T., et al. (2012). Severe dermatitis with loss of epidermal Langerhans cells in human and mouse zinc deficiency. J. Clin. Invest. *122*, 722–732.

Kull, I., Bergström, A., Melén, E., Lilja, G., van Hage, M., Pershagen, G., and Wickman, M. (2006). Early-life supplementation of vitamins A and D, in water-soluble form or in peanut oil, and allergic diseases during childhood. J. Allergy Clin. Immunol. *118*, 1299–1304.

Kunisawa, J., Gohda, M., Hashimoto, E., Ishikawa, I., Higuchi, M., Suzuki, Y., Goto, Y., Panea, C., Ivanov, , II, Sumiya, R., et al. (2013). Microbe-dependent $CD11b^+$ IgA plasma cells mediate robust early-phase intestinal IgA responses in mice. Nat Commun *4*, 1772.

Kurashima, Y., Kunisawa, J., Higuchi, M., Gohda, M., Ishikawa, I., Takayama, N., Shimizu, M., and Kiyono, H. (2007). Sphingosine 1-phosphate-mediated trafficking of pathogenic Th2 and mast cells for the control of food allergy. J. Immunol. *179*, 1577–1585.

Kurashima, Y., Amiya, T., Nochi, T., Fujisawa, K., Haraguchi, T., Iba, H., Tsutsui, H., Sato, S., Nakajima, S., Iijima, H., et al. (2012). Extracellular ATP mediates mast cell-dependent intestinal inflammation through P2X7 purinoceptors. Nat Commun *3*, 1034.

Lunderius-Andersson, C., Enoksson, M., and Nilsson, G. (2012). Mast Cells Respond to Cell Injury through the Recognition of IL-33. Front Immunol *3*, 82.

Masuda, A., Nakamura, A., Maeda, T., Sakamoto, Y., and Takai, T. (2007). Cis binding between inhibitory receptors and MHC class I can regulate mast cell activation. J. Exp. Med. *204*, 907–920.

Matsushima, H., Yamada, N., Matsue, H., and Shimada, S. (2004). TLR3-, TLR7-, and TLR9-mediated production of proinflammatory cytokines and chemokines from murine connective tissue type skin-derived mast cells but not from bone marrow-derived mast cells. J. Immunol. *173*, 531–541.

Mizumoto, N., Kumamoto, T., Robson, S.C., Sévigny, J., Matsue, H., Enjyoji, K., and Takashima, A. (2002). CD39 is the dominant Langerhans cell-associated ecto-NTPDase: modulatory roles in inflammation and immune responsiveness. Nat. Med. *8*, 358–365.

Morizane, S., Yamasaki, K., Kabigting, F.D., and Gallo, R.L. (2010). Kallikrein expression and cathelicidin processing are independently controlled in keratinocytes by calcium, vitamin D(3), and retinoic acid. J. Invest. Dermatol. *130*, 1297–1306.

Naik, S., Bouladoux, N., Wilhelm, C., Molloy, M.J., Salcedo, R., Kastenmuller, W., Deming, C., Quinones, M., Koo, L., Conlan, S., et al. (2012). Compartmentalized control of skin immunity by resident commensals. Science *337*, 1115–1119.

Nakamura, Y., Franchi, L., Kambe, N., Meng, G., Strober, W., and Núñez, G. (2012). Critical role for mast cells in interleukin-1β-driven skin inflammation associated with an activating mutation in the nlrp3 protein. Immunity *37*, 85–95.

Obata, T., Goto, Y., Kunisawa, J., Sato, S., Sakamoto, M., Setoyama, H., Matsuki, T., Nonaka, K., Shibata, N., Gohda, M., et al. (2010). Indigenous opportunistic bacteria inhabit mammalian gut-associated lymphoid tissues and share a mucosal antibody-mediated symbiosis. Proc. Natl. Acad. Sci. USA *107*, 7419–7424.

Okano, J., Lichti, U., Mamiya, S., Aronova, M., Zhang, G., Yuspa, S.H., Hamada, H., Sakai, Y., and Morasso, M.I. (2012). Increased retinoic acid levels through ablation of Cyp26b1 determine the processes of embryonic skin barrier formation and peridermal development. J. Cell Sci. *125*, 1827–1836.

Otsuka, A., Kubo, M., Honda, T., Egawa, G., Nakajima, S., Tanizaki, H., Kim, B., Matsuoka, S., Watanabe, T., Nakae, S., et al. (2011). Requirement of interaction between mast cells and skin dendritic cells to establish contact hypersensitivity. PLoS ONE *6*, e25538.

Sandig, H., and Bulfone-Paus, S. (2012). TLR signaling in mast cells: common and unique features. Front Immunol *3*, 185.

Sawaguchi, M., Tanaka, S., Nakatani, Y., Harada, Y., Mukai, K., Matsunaga, Y., Ishiwata, K., Oboki, K., Kambayashi, T., Watanabe, N., et al. (2012). Role of mast cells and basophils in IgE responses and in allergic airway hyperresponsiveness. J. Immunol. *188*, 1809–1818.

Schirmer, C., Klein, C., von Bergen, M., Simon, J.C., and Saalbach, A. (2010). Human fibroblasts support the expansion of IL-17-producing T cells via up-regulation of IL-23 production by dendritic cells. Blood *116*, 1715–1725.

Sudo, N., Tanaka, K., Koga, Y., Okumura, Y., Kubo, C., and Nomoto, K. (1996). Extracellular ATP activates mast cells via a mechanism that is different from the activation induced by the cross-linking of Fc receptors. J. Immunol. *156*, 3970–3979.

Takahashi, T., Kimura, Y., Niwa, K., Ohmiya, Y., Fujimura, T., Yamasaki, K., and Aiba, S. (2013). In vivo imaging demonstrates ATP release from murine keratinocytes and its involvement in cutaneous inflammation after tape stripping. J. Invest. Dermatol. *133*, 2407–2415.

Takano, H., Nakazawa, S., Okuno, Y., Shirata, N., Tsuchiya, S., Kainoh, T., Takamatsu, S., Furuta, K., Taketomi, Y., Naito, Y., et al. (2008). Establishment of the culture model system that reflects the process of terminal differentiation of connective tissue-type mast cells. FEBS Lett. *582*, 1444–1450.

Tsai, M., Grimbaldeston, M., and Galli, S.J. (2011). Mast cells and immunoregulation/immunomodulation. Adv. Exp. Med. Biol. *716*, 186–211.

Varani, J., Fligiel, H., Zhang, J., Aslam, M.N., Lu, Y., Dehne, L.A., and Keller, E.T. (2003). Separation of retinoid-induced epidermal and dermal thickening from skin irritation. Arch. Dermatol. Res. *295*, 255–262.

Wang, Z., MacLeod, D.T., and Di Nardo, A. (2012). Commensal bacteria lipoteichoic acid increases skin mast cell antimicrobial activity against vaccinia viruses. J. Immunol. *189*, 1551–1558.

Wilhelm, K., Ganesan, J., Müller, T., Dürr, C., Grimm, M., Beilhack, A., Krempl, C.D., Sorichter, S., Gerlach, U.V., Jüttner, E., et al. (2010). Graft-versus-host disease is enhanced by extracellular ATP activating P2X7R. Nat. Med. *16*, 1434–1438.

Xing, W., Austen, K.F., Gurish, M.F., and Jones, T.G. (2011). Protease phenotype of constitutive connective tissue and of induced mucosal mast cells in mice is regulated by the tissue. Proc. Natl. Acad. Sci. USA *108*, 14210–14215.

Yamasaki, K., Di Nardo, A., Bardan, A., Murakami, M., Ohtake, T., Coda, A., Dorschner, R.A., Bonnart, C., Descargues, P., Hovnanian, A., et al. (2007). Increased serine protease activity and cathelicidin promotes skin inflammation in rosacea. Nat. Med. *13*, 975–980.

Yokota, Y., Mansouri, A., Mori, S., Sugawara, S., Adachi, S., Nishikawa, S., and Gruss, P. (1999). Development of peripheral lymphoid organs and natural killer cells depends on the helix-loop-helix inhibitor Id2. Nature *397*, 702–706.

Regulation of Intestinal IgA Responses by Dietary Palmitic Acid and Its Metabolism

Jun Kunisawa,[*,†,‡,§,¶] Eri Hashimoto,[*,†] Asuka Inoue,[‡,‖] Risa Nagasawa,[*,†] Yuji Suzuki,[†] Izumi Ishikawa,[†] Shiori Shikata,[*,†] Makoto Arita,[#,**,1] Junken Aoki,[††,‖] and Hiroshi Kiyono[†,‡,††,‡‡,§§]

Enhancement of intestinal IgA responses is a primary strategy in the development of oral vaccine. Dietary fatty acids are known to regulate host immune responses. In this study, we show that dietary palmitic acid (PA) and its metabolites enhance intestinal IgA responses. Intestinal IgA production was increased in mice maintained on a PA-enriched diet. These mice also showed increased intestinal IgA responses against orally immunized Ag, without any effect on serum Ab responses. We found that PA directly stimulates plasma cells to produce Ab. In addition, mice receiving a PA-enriched diet had increased numbers of IgA-producing plasma cells in the large intestine; this effect was abolished when serine palmitoyltransferase was inhibited. These findings suggest that dietary PA regulates intestinal IgA responses and has the potential to be a diet-derived mucosal adjuvant. ***The Journal of Immunology*****, 2014, 193: 000–000.**

High levels of IgA are present in the intestine, where they protect the host against pathogenic microorganisms by preventing their attachment to and entrance into epithelial cells, as well as by neutralizing their toxins (1). Some patients with IgA deficiency show increased susceptibility to infectious pathogens, including *Giardia lamblia*, *Campylobacter*, *Clostridium*, *Salmonella*, and rotavirus (2). Given the immunologic importance of IgA in immunosurveillance in the intestine, the primary goal of effective oral vaccines is the efficient induction of Ag-specific IgA responses (3).

An efficient intestinal IgA response requires host-derived factors, including cytokines (e.g., IL-5, IL-6, IL-10, IL-15, APRIL, BAFF) and chemokines (e.g., CCL25/CCR9) (4, 5), as well as immunologic cross-talk with environmental factors (e.g., commensal bacteria and dietary materials) (6). Indeed, germ-free mice have decreased intestinal IgA responses because of the immature structure of Peyer's patches (PPs) and isolated lymphoid follicles (7, 8). We recently identified a unique subset of intestinal IgA-producing plasma cells (PCs) in the murine intestine; these cells expressed CD11b, required microbial stimulation and mature PP structure, proliferated vigorously, and produced high amounts of IgA (9).

In addition to commensal bacteria, nutritional molecules, such as vitamins, are essential for the development, maintenance, and regulation of intestinal immune responses (6, 10, 11). Therefore, nutritional deficiencies and inappropriate dietary intake increase the risk for infectious, allergic, and inflammatory diseases (12, 13). Among various dietary factors, oils are known to influence host immune function and inflammatory responses (14–16). Overnutrition due to a high-fat diet leads to the development of inflammation in adipose tissue, which is frequently associated with obesity and atherosclerosis (17). Recent findings suggest that, in addition to the quantity of oil ingested, the fatty acid (FA) composition of the oil is an important factor in various immunologic and inflammatory conditions (14–16). Dietary oil is generally composed of long-chain saturated FAs (e.g., C16:0 palmitic acid [PA] and C18:0 stearic acid) and mono- or polyunsaturated FAs (PUFAs; e.g., C18:1 oleic acid, C18:2 linoleic acid, and C18:3 α-linolenic acid). α-Linolenic acid and linoleic acid are precursors of ω3 and ω6 PUFAs, respectively; ω3 FAs are metabolized into anti-inflammatory molecules, whereas ω6 FAs are converted into proinflammatory lipid mediators (16, 18). Therefore, the ratio of α-linolenic acid/linoleic acid in dietary oils is thought to determine the onset of various immunologic conditions. In addition to modulating the ω3–ω6 PUFA balance, saturated FAs, such as PA, stimulate host immune responses by promoting the production of proinflammatory cytokines, including IL-6 and TNF-α (19, 20). Although these proinflammatory cytokines are prerequisite factors for the efficient induction of IgA

*Laboratory of Vaccine Materials, National Institute of Biomedical Innovation, Osaka 567-0085, Japan; †Division of Mucosal Immunology, Department of Microbiology and Immunology, The Institute of Medical Science, University of Tokyo, Tokyo 108-8639, Japan; ‡International Research and Development Center for Mucosal Vaccines, The Institute of Medical Science, University of Tokyo, Tokyo 108-8639, Japan; §Department of Microbiology and Immunology, Kobe University School of Medicine, Kobe 650-0017, Japan; ¶Graduate School of Pharmaceutical Sciences and Graduate School of Dentistry, Osaka University, Osaka 565-0871, Japan; ‖Laboratory of Molecular and Cellular Biochemistry, Graduate School of Pharmaceutical Sciences, Tohoku University, Sendai 980-8578, Japan; #Department of Health Chemistry, Graduate School of Pharmaceutical Sciences, University of Tokyo, Tokyo 113-0033, Japan; **Precursory Research for Embryonic Science and Technology, Japan Science and Technology Agency, Saitama 332-0012, Japan; ††Core Research for Evolutional Science and Technology, Japan Science and Technology Agency, Saitama 332-0012, Japan; ‡‡Department of Medical Genome Science, Graduate School of Frontier Science, University of Tokyo, Chiba 277-8561, Japan; and §§Graduate School of Medicine, University of Tokyo, Tokyo 113-0033, Japan

[1]Current address: Laboratory for Metabolomics, RIKEN Center for Integrative Medical Sciences, Yokohama, Kanagawa, Japan.

Received for publication November 1, 2013. Accepted for publication June 11, 2014.

This work was supported by grants from the Science and Technology Research Promotion Program for Agriculture, Forestry, Fisheries, and Food Industry (to J.K.); the Program for Promotion of Basic and Applied Research for Innovations in Bio-oriented Industry (to J.K.); the Ministry of Education, Culture, Sports, Science, and Technology of Japan (to J.K., M.A., J.A., and H.K.); the Ministry of Health and Welfare of Japan (to J.K. and H.K.); the Yakult Bio-Science Foundation (to J.K.); the Ono Medical Research Foundation (to J.K.); the Japan Science and Technology Agency, Core Research for Evolutional Science and Technology (to J.A. and H.K.); and Precursory Research for Embryonic Science and Technology (to M.A.).

Address correspondence and reprint requests to Dr. Jun Kunisawa, Laboratory of Vaccine Materials, National Institute of Biomedical Innovation, 7-9-8 Asagi Saito, Osaka 567-0085, Japan. E-mail address: kunisawa@nibio.go.jp

The online version of this article contains supplemental material.

Abbreviations used in this article: CT, cholera toxin; FA, fatty acid; iLP, intestinal lamina propria; PA, palmitic acid; PC, plasma cell; PP, Peyer's patch; PUFA, polyunsaturated fatty acid; S1P, sphingosine 1 phosphate; SPT, serine palmitoyltransferase.

www.jimmunol.org/cgi/doi/10.4049/jimmunol.1302944

responses (5), the immunologic function of dietary PA in the control of IgA production remained to be investigated. In this study, we show that PA-enriched diets enhance intestinal IgA responses both directly and through their metabolic pathways.

Materials and Methods

Mice

Female BALB/c, C3H/HeJ, and C3H/HeN mice were purchased from CLEA Japan (Tokyo, Japan). Chemically defined AIN-93M–based diets containing soybean, palm, or coconut oil or soybean oil plus supplemental purified PA were from Oriental Yeast (Tokyo, Japan). All mice were provided with a sterile diet and water ad libitum. To inhibit serine palmitoyltransferase (SPT) activity, mice were treated with myriocin (1.0 mg/kg i.p. daily; Sigma-Aldrich, St. Louis, MO) for 4 d (21). All mice were maintained in the experimental animal facility at the University of Tokyo and National Institute of Biomedical Innovation; the experiments were approved by the Animal Care and Use Committee of each institute and conducted in accordance with their guidelines.

Cell isolation

To isolate mononuclear cells from PPs, we stirred intestinal tissues in RPMI 1640 medium containing 2% FCS and 0.5 mg/ml collagenase (Wako, Osaka, Japan). Cells were isolated from the intestinal lamina propria (iLP) as previously described (9, 22). Briefly, PPs were removed, and small and large intestines were cut into 2-cm pieces, which were stirred in RPMI 1640 containing 1 mM EDTA and 2% FCS. Then the tissues were stirred in collagenase for 15 min three times (small intestine, 0.8 mg/ml; large intestine, 1.6 mg/ml) before undergoing discontinuous Percoll gradient centrifugation. Lymphocytes were isolated at the interface between the 40 and 75% layers.

Oral immunization

Mice received sodium bicarbonate to neutralize gastric acid before oral immunization (9, 22). Thirty minutes later, the mice were immunized orally concurrently with 1 mg OVA (Sigma-Aldrich) and 10 μg cholera toxin (CT; List Biological Laboratories, Campbell, CA). This oral-immunization procedure was conducted on days 0, 7, and 14.

Detection of total Ig by ELISA and OVA-specific Ab responses by ELISPOT assay

Total Ig levels in serum and fecal extracts were determined by ELISA, as previously described (9, 22). To measure Ab concentration, purified murine isotype-specific Abs (BD Biosciences, San Jose, CA) were used as standards for quantification. For the detection of OVA-specific Abs and Ab-forming cells, fecal extracts and iLP were prepared 7 d after the final immunization. Standard OVA-specific ELISAs and ELISPOT assays were performed as previously described (9, 22).

Flow cytometry and cell sorting

Flow cytometry and cell sorting were performed as previously described (9, 22). Cells were preincubated with anti-CD16/32 Ab and then stained with fluorescent Abs specific for B220, IgG1, IgA (all from BD Biosciences), CD19, and CD138 (BioLegend, San Diego, CA). Forward scatter–height and forward scatter–area discrimination was used to exclude doublet cells, and Via-Probe Cell Viability Solution (BD Biosciences) was used to discriminate between dead and living cells. For the BrdU-uptake assay, mice received 1 mg BrdU i.p., and the BrdU signal was detected according to the manufacturer's protocol (BD Biosciences) (9). Concentration-matched isotype Abs were used as negative controls. Flow cytometric analysis and cell sorting were carried out using FACSCanto II and FACSAria (BD Biosciences), respectively. We confirmed that cell purity was ~95%.

In vitro culture of PCs with PA

Stock solutions containing 5 mM PA and 10% BSA were prepared as previously reported (23). Purified IgA^+ $B220^-$ PCs isolated from the iLP (10^4 cells/well) or $CD19^+$ $CD138^+$ PCs isolated from the spleen (10^5 cells/well) were cultured with 10 or 100 μM PA for 96 h. The amount of IgA (for iLP) or IgG (for spleen) in the culture supernatant was determined by ELISA, as described earlier.

Measurement of PA in the serum and intestinal tissues

Lipids were extracted from serum and intestinal tissues by using chloroform–methanol and chloroform solutions. The specimens were dried in nitrogen gas and dissolved in 0.4 M potassium methoxide in methanol and 14% boron trifluoride in methanol. The FA concentrations in the solutions were measured (SRL, Tokyo, Japan) using gas chromatography (model GF 17A; Shimazu, Kyoto, Japan).

Statistics

Experimental groups were compared using the Mann–Whitney *U* test (GraphPad, San Diego, CA).

Results

Mice maintained on a diet containing palm oil show enhanced intestinal IgA production

To examine whether dietary PA affects intestinal IgA production, we maintained mice on a diet containing 4% soybean (control) or palm (PA-rich) oil for 2 mo (Fig. 1A) and measured the amounts of fecal IgA. Intestinal IgA production was higher in the mice that received palm oil than in those given soybean oil (Fig. 1B). In contrast, the amounts of serum IgG and IgA were similar between the soybean and palm oil groups (Fig. 1B, Supplemental Fig. 1). Palm oil is high in both PA and oleic acid (Fig. 1A), but mice maintained on a diet containing rapeseed oil, which contained a similar amount of oleic acid as that present in the palm oil, showed no enhancement of intestinal IgA production (data not shown).

We then considered whether other saturated FAs enhance intestinal IgA production. To this end, we used coconut oil, which (like palm oil) is a Palmae plant–based oil but contains large

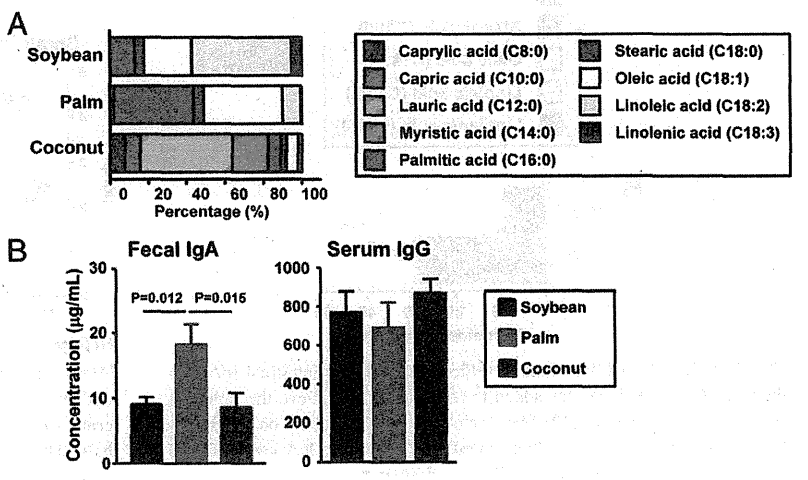

FIGURE 1. Palm oil enhances intestinal IgA production. (**A**) FA composition of soybean, palm, and coconut oils. (**B**) Mice were maintained on a diet containing soybean, palm, or coconut oil for 2 mo. Feces and serum samples were collected for measurement of the amounts of IgA and IgG, respectively (mean ± 1 SD, n = 10/group).

amounts of other saturated FAs, including lauric and myristic acids (Fig. 1A). Unlike palm oil, coconut oil did not alter fecal or serum Ab production in the mice (Fig. 1B). These findings suggest that dietary PA uniquely enhances intestinal IgA production.

PA-enriched dietary oils enhance intestinal IgA production and IgA responses against oral vaccine Ag

To confirm that PA enhances intestinal IgA production, we added PA to soybean oil to adjust its PA concentration to that of palm oil (Fig. 2A, *upper bar*). Fecal IgA levels in mice maintained for 2 mo on a diet containing the PA-enriched soybean oil were increased similarly to those of mice fed a palm oil–containing diet, but serum IgA production was unchanged (Fig. 2A, *lower bar*, Supplemental Fig. 1). These data suggest that PA is a key FA in the enhancement of intestinal IgA production.

We then investigated whether the enhanced production of intestinal IgA induced by dietary PA is reflected in the responses to an orally administered vaccine. To this end, we orally immunized mice concurrently with OVA and the mucosal adjuvant CT. In agreement with levels of naturally produced IgA, OVA-specific fecal IgA responses were enhanced in mice maintained on a diet that contained palm oil (Fig. 3). In addition, similarly increased OVA-specific IgA production was noted in mice maintained on PA-enriched soybean oil (Fig. 3). These findings suggest that dietary PA enhanced not only naturally produced intestinal IgA but also Ag-specific intestinal IgA induced by oral immunization.

PA content is increased in the intestinal, but not systemic, compartment

We next measured the amounts of PA in the intestines and serum of the mice. PA concentrations in the small and large intestines were higher in the mice maintained on PA-rich soybean oil compared with soybean oil alone (Fig. 4). In contrast, PA amounts in serum were comparable between groups (Fig. 4). These findings indicate that dietary PA affects the amount of PA locally in the intestine without any influence on serum PA concentration.

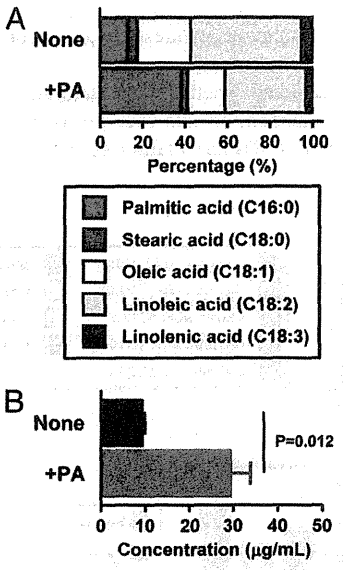

FIGURE 2. Dietary PA alone is sufficient to enhance intestinal IgA production. (**A**) Purified PA was added to soybean oil to achieve the same PA content as that in palm oil. (**B**) Mice were maintained for 2 mo on a diet containing soybean oil, with or without supplemental PA. The IgA levels of fecal extracts were measured (mean ± 1 SD, n = 16/group).

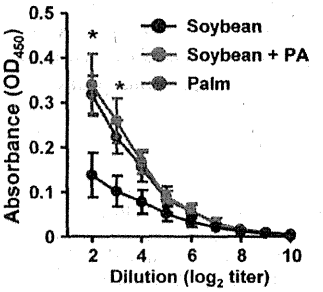

FIGURE 3. Ingestion of PA-enriched oil enhances intestinal IgA responses against orally immunized Ag. After mice were maintained for 2 mo on a diet containing soybean oil, soybean oil + PA, or palm oil, they were orally immunized with OVA plus CT on days 0, 7, and 14. On day 21, fecal extracts were collected for the determination of OVA-specific intestinal IgA by ELISA. Data are mean ± 1 SD (n = 4/group), and similar results were obtained from two independent experiments. *$p < 0.05$.

PA directly stimulates intestinal PCs to produce IgA

We then examined whether PA directly affected IgA production from PCs. To address this issue, we purified IgA^+ PCs from the intestine and cultured them with PA for 4 d. The amount of IgA in the intestinal PC culture supernatants increased in a dose-dependent manner (Fig. 5A). ELISPOT assays showed that PA did not increase the number of IgA-forming cells (Fig. 5B), suggesting that PA instead enhances Ab production from PCs. In addition, IgG production from $CD19^+$ $CD138^+$ PCs from the spleen was increased in the presence of PA (Supplemental Fig. 2), indicating that PA enhances Ab production, regardless of the Ig subtype.

PA acts as a ligand for TLR4 (24), prompting our investigation into whether TLR4 mediated the PA-induced direct activation of IgA PCs. To address this issue, we used C3H/HeN and C3H/HeJ mice. Although TLR4-mediated signaling differs between these two strains because of a spontaneous point mutation in the *Tlr4* gene of the C3H/HeJ mice (25, 26), intestinal PCs from these mouse strains produced identical levels of PA-induced IgA (Fig. 5C). Therefore, the direct effect of PA on IgA production from PCs likely is independent of the TLR4 pathway.

The PA-induced increase in IgA PCs in the large intestine is dependent on SPT

We used flow cytometry to determine the frequency of IgA^+ PCs in the small and large intestines. Although no significant difference between the control and PA-enriched diets was noted in the small intestine, the frequency of IgA^+ $B220^-$ PCs was increased in the

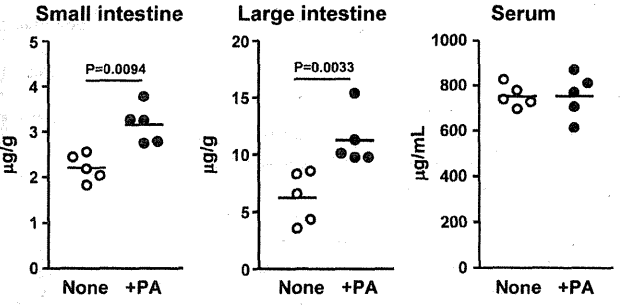

FIGURE 4. Increased PA content in the intestine of mice maintained on PA-enriched oils. Mice were maintained for 2 mo on a diet containing soybean oil, with or without PA, and small and large intestinal tissues and serum were collected for measurement of their PA contents. The graphs show data from individual mice, and the horizontal lines indicate the means; similar results were obtained from two independent experiments.

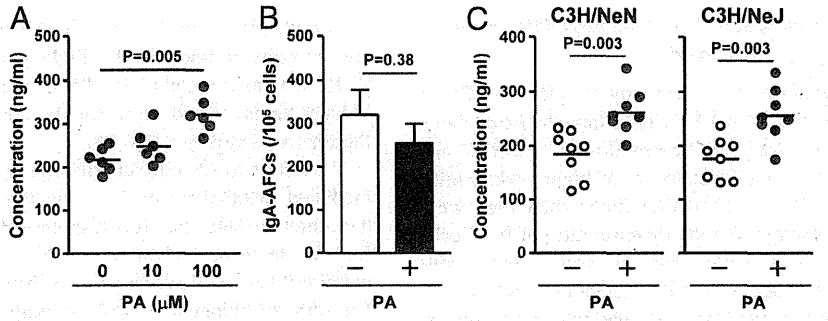

FIGURE 5. PA directly stimulates IgA-producing PCs via a TLR4-independent mechanism. IgA^+ $B220^-$ PCs were isolated from the small intestine of BALB/c (**A** and **B**) and C3H/HeN or C3H/HeJ mice (**C**) and cultured with 10 or 100 μM (A) or 100 μM (B and C) PA. The amount of IgA in the culture supernatant (A and C) and the number of IgA^+ Ab–forming cells (IgA^+-AFCs) (B) were determined by ELISA and ELISPOT, respectively. The graphs show data from individual samples, and the horizontal lines indicate the means; similar results were obtained from two independent experiments (A and C). Data in (B) are mean ± 1 SD (n = 10/group from two separate experiments).

large intestine of the PA-enriched diet group (Fig. 6A). Similarly, the number of OVA-specific IgA-forming cells was increased in the large, but not small, intestine of mice receiving oral immunization and the PA-enriched diet (Fig. 6B). In agreement with the lack of a PA-associated effect on small intestinal IgA, B cell differentiation into IgA^+ cells in the PPs, a lymphoid tissue for the initiation of small intestinal IgA responses (3), was unchanged in mice maintained on a PA-enriched diet (Supplemental Fig. 3).

PA can be converted into sphingolipids, including ceramide, sphingosine, and sphingosine 1 phosphate (S1P) (Fig. 6C); all of these lipids all known to promote cell proliferation, survival, and trafficking (27, 28). Therefore, we supposed that these PA-derived sphingolipids might be involved in the regulation of intestinal IgA PCs in the large intestine. To test this possibility, mice were treated with myriocin, an inhibitor of SPT, which is a key enzyme in the conversion of PA into sphingolipids (Fig. 6C). The PA-mediated increase in IgA PCs did not occur in the large intestine of mice that received myriocin (Fig. 6D), and myriocin had little effect on the number of $IgG1^+$ cells in the spleen (Supplemental Fig. 4), suggesting that SPT activity is required for this effect on large intestinal IgA PCs.

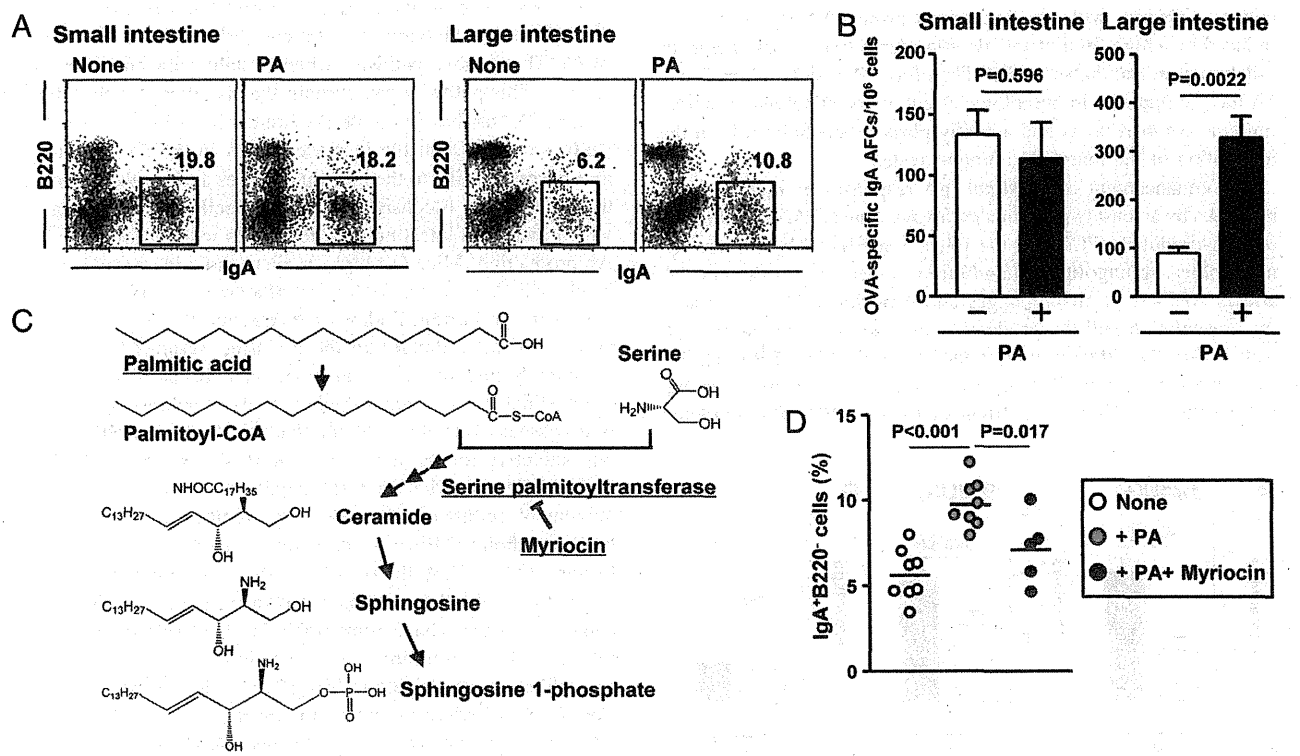

FIGURE 6. SPT is required for the increased number of IgA PCs in the large intestine. Mice were maintained on a diet containing soybean oil, with or without PA, for 2 mo. (**A**) Mononuclear cells were isolated from the small and large intestines for the flow cytometric analysis of IgA^+ $B220^-$ PCs. Data are representative of three independent experiments. (**B**) Mice were orally immunized with OVA plus CT on days 0, 7, and 14. On day 21, mononuclear cells were isolated from the small and large intestine for the detection of OVA-specific IgA Ab–forming cells by ELISPOT assay. Data are mean ± 1 SD (n = 6/group from two separate experiments). (**C**) The metabolic pathway mediated by SPT to generate sphingolipids from PA. (**D**) The frequency of IgA^+ $B220^-$ PCs in the large intestine of mice maintained on a PA-enriched diet and myriocin. The graphs show data from individual samples, and the horizontal lines indicate the means. Similar results were obtained from two independent experiments.

The increased proliferation of IgA PCs in the large intestine of mice maintained with a PA-enriched diet

We performed BrdU-uptake assays to examine the effects of PA on the proliferation and survival of IgA PCs in the large intestine. Soon after BrdU administration (day 1), the proportions of $BrdU^+$ and $BrdU^-$ IgA^+ cells in the large intestine were higher when mice were maintained on a PA-enriched diet than when they were maintained on the control diet, but the increase ratio of IgA^+ cells was higher in $BrdU^+$ IgA^+ cells than in $BrdU^-$ IgA^+ cells (Fig. 7A). These findings suggest that PA metabolites induced the proliferation of IgA^+ cells in the large intestine. In contrast, on day 4, both the control and PA-enriched groups showed similar levels of $BrdU^+$ IgA^+ cells (Fig. 7B). These data collectively suggested that PA metabolites primarily induced the proliferation of IgA^+ cells in the large intestine rather than prolonged their survival.

Discussion

In the current study, we extended our knowledge of lipid-mediated immune regulation by showing the immunologic function of dietary PA in the enhancement of intestinal IgA responses. Unlike the sterile environment of systemic immune compartments (e.g., spleen), intestinal tissues are continuously exposed to exogenous factors, including commensal bacteria and dietary materials and actively use them to establish a homeostatic inflammatory condition (6). Indeed, in contrast to the massive inflammatory responses induced by the systemic injection of bacterial products, such as LPS (e.g., sepsis), the intestinal immune system requires bacterial stimulation for its maturation (29). Our current study demonstrates that dietary PA can augment intestinal IgA responses when an appropriate amount of dietary oil (4%) is supplied. This effect contrasts sharply with the deleterious plasma PA levels that are induced by a high-fat diet and are considered to be a risk factor for inflammation and diabetes (30). Therefore, like bacterial products, PA has the opposite immunologic effect on intestinal and systemic immune compartments and actually plays a beneficial role in the maturation of the intestinal immune system.

The enhancement of intestinal IgA responses by dietary PA is mediated by at least two distinct pathways. One is PA's direct effect on IgA-producing PCs, and the other is mediated by PA-derived metabolites, sphingolipids. In addition to these two pathways, PA affects APCs (e.g., macrophages and dendritic cells) to promote Ag presentation and the production of cytokines, including IL-6 and TNF-α; this effect is at least partly mediated by TLR4 (31, 32) and represents a plausible third pathway to enhancing intestinal IgA production. Unlike the effect of PA on APCs, PA promoted IgA production from PCs in a TLR4-independent manner in our current study. In line with this finding, several groups reported that TLR2 acts as a receptor for PA or that PA enters cells where it induces signal transduction for the consequent production of inflammatory cytokines (33–36).

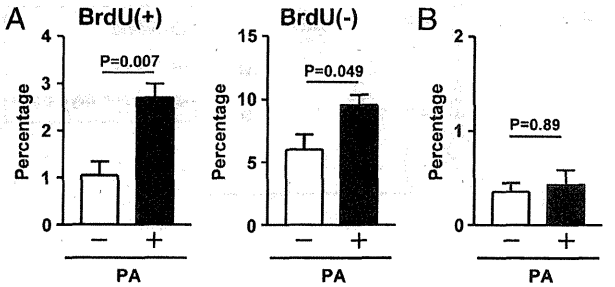

FIGURE 7. A PA-enriched diet induces the proliferation of IgA PCs. Mice were maintained on a diet containing soybean oil, with or without PA, for 2 mo, after which BrdU was injected i.p. (day 0). On day 1 (**A**) and day 4 (**B**), mononuclear cells isolated from the large intestine were analyzed by flow cytometry to determine the proportion of $BrdU^+$ IgA^+ PCs. Data are mean ± 1 SD (n = 4). Similar results were obtained from two independent experiments.

In addition to PA's direct effect on IgA-producing PCs, the SPT-mediated metabolism of PA is involved in the PA-mediated enhancement of intestinal IgA responses. SPT is an essential enzyme for the de novo pathway of sphingolipid synthesis, in which palmitoyl-CoA and serine act as substrates of SPT to generate 3-keto-dihydosphingosine, with subsequent conversion into other sphingolipids, such as sphingomyelin, ceramide, sphingosine, and S1P (37, 38). Sphingolipids are a class of membrane lipids that also are known to have biologic functions (27, 28). For example, ceramide regulates cytoskeletal changes, cell cycle, and apoptosis (27, 28). Accordingly, perhaps an increase in ceramide concentrations induced the proliferation or prolonged the survival of IgA PCs, subsequently increasing the number of IgA-producing PCs in the large intestine. In addition, in the extracellular compartment, S1P controls cell trafficking by recruiting cells toward regions with high concentrations of S1P (39). Of note, we previously reported that S1P regulates intestinal IgA responses by controlling trafficking of IgA^+ cells from inductive sites (e.g., PPs and peritoneal cavity) into the iLP (22, 40). Therefore, another possibility is that the PA-enriched diet induced an increase in the intestinal extracellular S1P concentration, resulting in the effective recruitment of IgA PCs into the intestine. Our current findings suggest that at least one of the enhancing effects of the PA-enriched diet was mediated by the induction of proliferating IgA^+ PCs in the large intestine.

PA was not only included in the diet but was also generated through de novo lipogenesis, whereby carbohydrates are converted to PA. The de novo pathway achieves stable concentrations of PA in vivo. This pathway can explain the specificity of the effect of dietary PA enrichment on the PA content in various tissues. In this study, we found that the increases in PA in the PA-enriched diet group were specific to the intestinal tissues and not the serum. This tissue specificity is consistent with the specific effect of dietary PA, which increased intestinal IgA responses without affecting serum Ab production. Mice fed high-fat diets show increased serum PA levels, which are a risk factor for inflammation and diabetes (30). However, our current findings indicate that the increased proportion of PA in the dietary oil did not affect serum PA levels when the overall amount of oil consumed was normal (4%).

Intestinal tissues contain higher levels of sphingolipids than do other tissues (41), and we found that the effect of an SPT inhibitor was selective for the large, but not small, intestine. One of the major differences between the small and large intestines is the amount of commensal bacteria. We recently reported that some lipid metabolic pathways are uniquely mediated by commensal bacteria (42), raising the possibility that commensal bacteria may affect sphingolipid metabolism. However, germ-free and specific pathogen–free rats have comparable levels of sphingolipids in the intestine (43). Therefore, it is plausible that commensal bacteria are unlikely to participate in this pathway. In contrast, the expression pattern of enzymes involved in the generation of sphingolipids differs between intestinal compartments (44, 45), indicating that the differences in sphingolipid metabolism between the small and large intestines determine their differing dependence on SPT in PA-mediated intestinal IgA responses.

Taken together, our current findings demonstrate that dietary PA and its metabolites play a critical role in the enhancement of intestinal IgA responses. This information can be applied to the development of mucosal adjuvants.